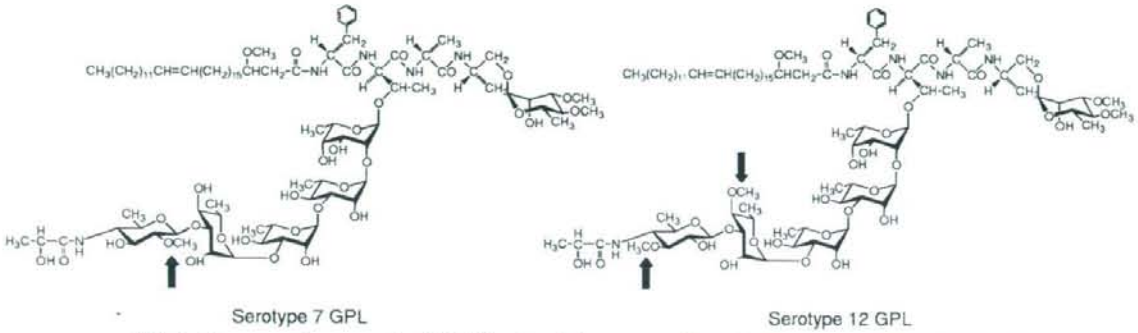

FIG. 1. Structures of serotype 7 and 12 GPLs. *O*-methyl groups specific to the serotypes are indicated by arrows.

In a previous study, we determined the complete structure of the GPL derived from *M. intracellulare* serotype 7 and characterized the serotype 7-specific gene cluster for GPL synthesis (10). The structure of serotype 7 GPL closely resembles that of serotype 12 GPL, except for O methylation (Fig. 1). In the present study, we determined the nucleotide sequence of the serotype 12-specific gene cluster involved in the glycosylation of the GPL and characterized two novel open reading frames (ORFs) encoding *O*-methyltransferases that determine the difference of serotype 12 GPL from serotype 7 GPL.

MATERIALS AND METHODS

Bacterial strains and construction of *M. intracellulare* cosmid library. *M. intracellulare* serotype 12 strain ATCC 35762 (NF 103), *M. intracellulare* serotype 7 strain ATCC 35847 (NF 027), and *M. intracellulare* serotype 7 strain NF 112 were used for this study. A cosmid library of *M. intracellulare* NF 103 was constructed as described previously (10). Briefly, genomic DNA of *M. intracellulare* NF 103 was prepared by mechanical disruption of bacterial cells in phosphate-buffered saline containing 50 mM EDTA, followed by phenol-chloroform extraction and precipitation with ethanol. Genomic DNA fragments randomly sheared to 30-kb to 50-kb fragments during the extraction process were fractionated and electroeluted from agarose gels. These DNA fragments were ligated to dephosphorylated arms of pYUB412 (XbaI-EcoRV and EcoRV-XbaI). After in vitro packaging using Gigapack III Gold extracts (Stratagene, La Jolla, CA), recombinant cosmids were introduced into *Escherichia coli* STBL2.

Isolation of cosmid clones carrying the GPL biosynthesis gene cluster and sequence analysis. PCR was used to isolate cosmid clones carrying the rhamnosyltransferase gene (*rtfA*), using primers rtfA-F (5′-TTTTGGAGCGACGAGTTCAT C-3′) and rtfA-R (5′-GTGTAGTTGACCACGCCGAC-3′). The insert of cosmid clone 161 was sequenced using a kit (BigDye Terminator cycle sequencing kit, version 3.1; Applied Biosystems, Foster City, CA) and a sequence analyzer (ABI Prism 310; Applied Biosystems). The putative function of each ORF was identified by similarity searches between the deduced amino acid sequences and those of known proteins, using BLAST (http://www.ncbi.nlm.nih.gov/BLAST/) and FramePlot (http://www.nih.go.jp/~jun/cgi-bin/frameplot.pl) with the DNASIS computer program (Hitachi Software Engineering, Yokohama, Japan).

Transformation of *M. intracellulare*. PCR was used to amplify and clone *orfA* and *orfB* into the plasmid vector pVV16. *M. intracellulare* NF 027 and NF 112 were transformed with the resultant plasmids by electroporation. Primers used to amplify *orfA*, *orfB*, and *orfA-orfB* were orfA-F (5′-GCGGATCCAGTGTGCAG ACGAGCGGAACT-3′), orfA-R (5′-GCGAATTCTTATCGAGAAAAAATA AAAG-3′), orfB-F (5′-GCGGATCCACTGCTAGACTCCGCCACCAT-3′), and orfB-R (5′-GCGAATTCCTACACCTTCACGGCGAGTC-3′).

Preparation of GPLs and OSE moieties. GPL 7 and GPL 12 were purified from *M. intracellulare* NF 027 and NF 103, respectively. The preparation of GPLs was performed as described previously (10, 15, 17). Briefly, each strain was grown in Middlebrook 7H9 broth (Difco Laboratories, Detroit, MI) with 0.5% glycerol and 10% Middlebrook oleic acid-albumin-dextrose-catalase enrichment (Difco Laboratories) at 37°C for 2 to 3 weeks. The heat-killed bacteria were sonicated and extracted using chloroform-methanol (2:1 [vol/vol]). The extractable lipids were hydrolyzed with 0.2 N sodium hydroxide in methanol at 37°C for 2 h. After neutralization using 6 N hydrochloride, chloroform-methanol (2:1 [vol/vol]) and water were added. The organic phase containing alkaline-stable lipids was recovered and evaporated, with subsequent addition of acetone to remove any acetone-insoluble components. The supernatant was dried up. It was then treated using a Sep-Pak silica cartridge (Waters Corp., Milford, MA) with washing (chloroform-methanol [95:5 {vol/vol}]) and elution (chloroform-methanol [1:1 {vol/vol}]) for partial purification. The GPL was then purified completely by preparative thin-layer chromatography (TLC) with silica gel G (Uniplate; 20 cm × 20 cm × 250 μm; Analtech, Inc., Newark, DE). The TLC was developed repeatedly, using chloroform-methanol-water (60:16:2 [vol/vol/vol]), until a single spot was obtained. To prepare the OSE moiety, purified GPL was processed using β-elimination with alkaline borohydride, and then the carbohydrate chain moiety

TABLE 1. Similarity of Orfs in *M. intracellulare* serotype 12 strain ATCC 35762 to known protein sequences

Orf	Predicted molecular mass (Da)	Predicted pI	Similar protein	Identity (no. of matched amino acids/total no. of amino acids)	E value	GenBank accession no.
GtfB	45,830	6.87	Glycosyltransferase GtfB	412/418	0.0	BAF45360
Orf1	45,203	6.10	Putative glycosyltransferase	414/417	0.0	BAF45361
OrfA	28,904	7.42	Putative methyltransferase	182/224	5e−88	NP_218045
OrfB	29,930	5.15	Putative methyltransferase	102/204	1e−19	EAZ88812
Orf3	32,151	10.41	Putative glycosyltransferase	196/223	1e−108	BAF45363
Orf4	40,742	5.41	Putative aminotransferase	338/374	0.0	BAF45364
Orf5	35,812	5.26	Hypothetical protein	303/329	4e−162	BAF45365
Orf7	27,693	5.99	Putative metallophosphoesterase	223/241	1e−122	BAF45367
Tn	28,538	11.85	Putative transposase	213/255	6e−107	AAL61662
Orf8	80,044	9.16	Putative acyltransferase	689/747	0.0	BAF45368
Orf9	37,797	8.26	Putative glycosyltransferase	310/337	7e−169	BAF45369
DrrC	28,549	12.01	Daunorubicin resistance protein C	261/263	3e−141	BAF45370

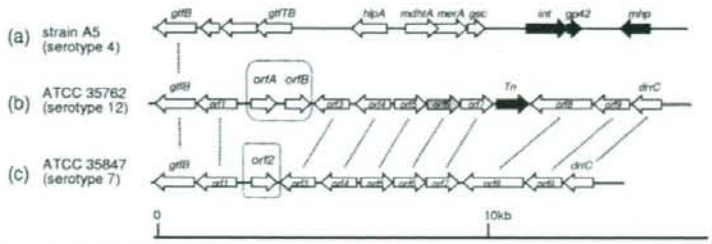

FIG. 2. Comparison of genetic organization of GPL biosynthesis clusters. (a) *M. avium* strain A5 organization, based on the annotated sequence obtained from GenBank (accession no. AY130970). (b) *M. intracellulare* ATCC 35762 (NF 103), sequenced in this study. (c) *M. intracellulare* ATCC 35847 (NF 027), sequenced in our previous study (GenBank accession no. AB274811). The orientation of each gene is shown by the arrow direction. The black arrows represent mobile elements, and the gray arrow represents a pseudogene. Mutually homologous ORFs and sequences are indicated with dotted lines.

elongated from D-*allo*-Thr was released as described previously (10, 15). Briefly, GPL was treated with 5 mg/ml sodium borohydride or borodeuteride in 0.5 N sodium hydroxide-ethanol (1:1 [vol/vol]) at 60°C for 16 h, with stirring. The reaction mixture was decationized with Dowex 50W X8 beads (The Dow Chemical Company, Midland, MI). The supernatant was collected and evaporated under nitrogen to remove boric acid. The dried residue was partitioned into two layers, using chloroform-methanol (2:1 [vol/vol]) and water. The upper aqueous phase was recovered and evaporated. In these processes, the OSE was purified as an oligoglycosyl alditol.

MALDI-TOF MS and MALDI-TOF/TOF MS analyses. The molecular species of the intact GPLs were detected using matrix-assisted laser desorption ionization–time-of-flight mass spectrometry (MALDI-TOF MS) with an Ultraflex II spectrophotometer (Bruker Daltonics, Billerica, MA). Each GPL was dissolved in chloroform-methanol (2:1 [vol/vol]) at a concentration of 1 mg/ml; 1 μl of a sample was then applied directly to the sample plate, followed by the addition of 1 μl of 10-mg/ml 2,5-dihydroxybenzoic acid in chloroform-methanol (1:1 [vol/vol]) as a matrix. The intact GPL was analyzed in the reflectron mode, with an accelerating voltage operating in positive mode at 20 kV (3). The OSE was analyzed by the fragment pattern with MALDI-TOF/TOF MS to determine the glycosyl composition. The OSE was dissolved with ethanol-water (3:7 [vol/vol]); the matrix was 10 mg/ml 2,5-dihydroxybenzoic acid in ethanol-water (3:7 [vol/vol]). The OSE and matrix were added to the sample plate by the same method as that for intact GPL. They were then analyzed in the lift-lift mode.

GC-MS analyses of alditol acetate derivatives. Gas chromatography (GC) and GC-MS analyses of partially methylated alditol acetate derivatives were performed to determine glycosyl compositions and linkage positions. Perdeuteromethylation was conducted using a modified procedure of Hakomori, as described previously (10, 11). Briefly, the dried OSE was dissolved with a mixture of dimethyl sulfoxide and sodium hydroxide, and deuteromethyl iodide was added. The reaction mixture was stirred at room temperature for 15 min, followed by the addition of water and chloroform. After centrifugation at 2,400 × *g* for 15 min, the upper water layer was discarded. The chloroform layer was washed twice with water and evaporated completely. To prepare partially deuteromethylated alditol acetates, perdeuteromethylated OSE was hydrolyzed using 2 N trifluoroacetic acid at 120°C for 2 h, reduced with 10 mg/ml sodium borodeuteride at 25°C for 2 h, and acetylated with acetic anhydride at 100°C for 1 h (6, 10, 16). GC-MS was then performed using a benchtop ion-trap mass spectrometer (Trace DSQ GC/MS; Thermo Electron Corporation, Austin, TX) equipped with a fused capillary column (30 m; 0.25-mm internal diameter) (Equity-1 or SP-2380; Supelco, Bellefonte, PA). Helium was used as the carrier gas, and the flow rate was 1 ml/min. The SP-2380 column was used for the analysis of alditol acetate derivatives. The temperature program was started at 60°C, with an increase of 40°C/min to 260°C and a hold at 260°C for 25 min. The Equity-1 column was used for analysis of perdeuteromethylated alditol acetate derivatives. The temperature program was 80°C for 1 min, with an increase of 20°C/min to 180°C followed by an increase of 8°C/min to 280°C.

Nucleotide sequence accession number. The nucleotide sequence reported here has been deposited in the NCBI GenBank database under accession number AB353739.

RESULTS

Cloning and sequence of the serotype 12 GPL biosynthesis cluster. To isolate the serotype 12-specific GPL biosynthesis gene cluster, a genomic cosmid library of an *M. intracellulare* serotype 12 strain, NF 103, was constructed. DNA was extracted from each clone by boiling. Using colony PCR with *rfbA* primers, the positive clone 161 was isolated from the *E. coli* transductants. Sequencing analysis revealed that cosmid clone 161 carried the DNA region from *gtfB* to *drrC*. Ten ORFs and one pseudogene other than *gtfB* and *drrC* were observed in the cluster (Table 1 and Fig. 2). The genetic organization between the *gtfB* and *drrC* genes (15.6 kb) of *M. intracellulare* NF 103 (serotype 12) closely resembled that of

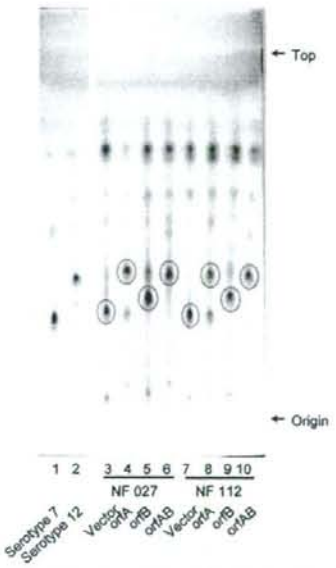

FIG. 3. TLC patterns of alkaline-stable lipids derived from *M. intracellulare* serotype 7 transformants. GPL 7 and GPL 12 were purified from *M. intracellulare* serotype 7 strain ATCC 35847 (NF 027) and serotype 12 strain ATCC 35762 (NF103). TLC was developed with a solvent system of chloroform-methanol-water (65:25:4 [vol/vol/vol]). Circled spots indicate prominent GPLs.

the same region of *M. intracellulare* NF 027 (serotype 7), except for three loci (Fig. 2). The first difference between them was an additional ORF encoding a transposase between *orf7* and *orf8* in NF 103 (Fig. 2). The second difference was that the *orf6* homologous sequence in NF 103 had a frame shift, indicating that this locus does not encode a protein. The third difference is that two novel ORFs (*orfA* and *orfB*) instead of *orf2* were found between *orf1* and *orf3* in NF 103.

Functional analysis of the two unique ORFs found in the serotype 12 GPL biosynthesis cluster. Based on sequence homology, *orfA* and *orfB* were able to encode methyltransferases responsible for producing serotype 12 GPLs (Table 1). We constructed three plasmids carrying *orfA* and/or *orfB* downstream of the *hsp-60* promoter to test this. These plasmids and a control vector plasmid were introduced individually into *M. intracellulare* serotype 7 (NF 027 and NF 112), and transformants were obtained. The GPLs produced from each transformant were analyzed.

The alkaline-stable lipids derived from six transformants of NF 027 and NF 112 in addition to the control strains (vector only) were developed by TLC, and the produced GPLs were compared to the spots of GPL 7 and GPL 12 (Fig. 3). The R_f values for GPLs synthesized in NF 027 transformed with *orfA* and NF 027 transformed with *orfA* and *orfB* (GPL 7-orfA and GPL 7-orfAB, respectively) were almost identical to that for GPL 12; the R_f value for the GPL synthesized in NF 027 transformed with *orfB* (GPL 7-orfB) was intermediate between those of GPL 7 and GPL 12, although the GPL synthesized in the control strain (GPL vector) was not changed from GPL 7. These results suggest that *orfA*, *orfB*, and *orfA-orfB* introduced into serotype 7 strain NF 027 were expressed and that they functioned for the modification of GPLs. We investigated the structural definition of these modified GPLs.

The GPLs produced in the transformants were purified using preparative TLC; their molecular weights were measured using MALDI-TOF MS (Fig. 4). The main molecularly related ions of GPL 7 and GPL 12 were detected as *m/z* 1,897 and 1,911, respectively, for $[M + Na]^+$ (Fig. 4a and b). The predominant *m/z* values were 1,911 for GPL 7-orfA, 1,897 for GPL 7-orfB, and 1,911 for GPL7-orfAB (Fig. 4c to e). The molecular weight of GPL 7-orfB was the same as that of GPL 7, and those of GPL 7-orfA and GPL 7-orfAB were equal to that of GPL 12. Next, MALDI-TOF/TOF MS analysis was performed to determine the glycosyl pattern, using fragment ions of glycosyl cleavage. The fragment ions of the GPL vector (equal to GPL 7) showed *m/z* 254, 400, 546, and 692 for cleavage in turn from terminal 4*N*-acyl-hexose (Hex) and 336, 482, and 628 for cleavage in the opposite direction from 6-d-Tal (Fig. 5a). The fragment ions of GPL 7-orfA, *m/z* 414 and 642, were different from those of GPL 7, i.e., *m/z* 400 and 628, respectively; they demonstrated that the mass number of the sugar next to the terminal Hex increased 14 mass units (Fig. 5b). This result suggests that the second sugar from the terminal one was changed from Rha to *O*-methyl rhamnose (*O*-Me-Rha). Similarly, the fragment pattern of GPL 7-orfAB was identical to that of GPL 7-orfA, although that of GPL 7-orfB was the same as that of GPL 7 (Fig. 5c and d). Altogether, GPL 7-orfAB was predicted to have a modification of the *O*-Me position in the terminal Hex along with the substitution of *O*-Me-Rha for Rha in the sugar next to the terminal Hex; GPL 7-orfB was modified only at the *O*-Me position in the terminal Hex.

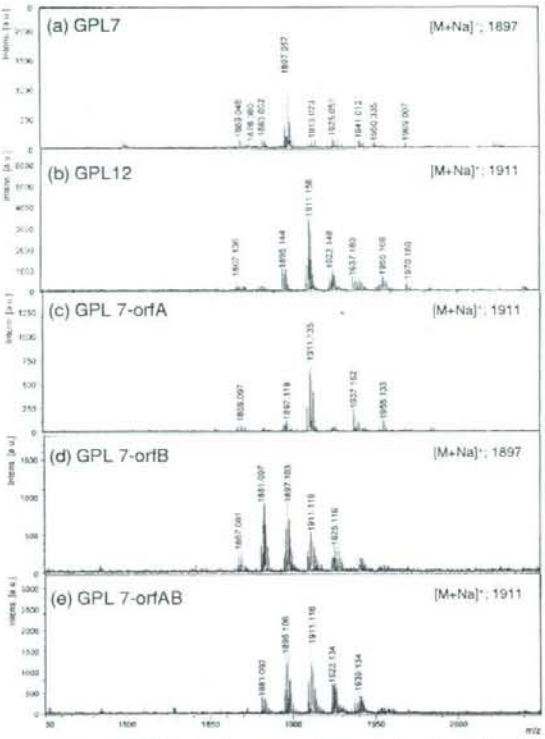

FIG. 4. MALDI-TOF MS spectra of GPLs derived from *M. intracellulare* serotype 7, serotype 12, and serotype 7 transformants. a.u., absorbance units.

GC-MS analyses of alditol acetate and perdeuteromethyl alditol acetate derivatives were performed to assign the linkage position of *O*-Me. As portrayed in Fig. 6a and b, the alditol acetate derivatives of the second sugar from the terminal 4*N*-acyl-Hex in GPL 7-orfA and GPL 7-orfB were assigned to 1,2,3,5-tetra-acetyl-4-*O*-methyl-rhaminitol (*m/z* 99, 131, 159, 201, and 261) and 1,2,3,4,5-penta-acetyl-rhaminitol (*m/z* 115, 157, 187, 217, 231, 289, and 303), respectively. The perdeuteromethyl alditol acetate derivatives of the terminal sugar in GPL 7-orfA and GPL 7-orfB were assigned to 3-*O*-deuteromethyl-1,5-di-*O*-acetyl-4-2′-*O*-deuteromethyl-propanoyl-deuteromethylamido-4,6-dideoxy-2-*O*-methyl-hexitol (*m/z* 105, 118, 165, 209, 222, 269, and 300) and 2-*O*-deuteromethyl-1,5-di-*O*-acetyl-4-2′-*O*-deuteromethyl-propanoyl-deuteromethyl-amido-4,6-dideoxy-3-*O*-methyl-hexitol (*m/z* 105, 121, 165, 206, 222, 266, and 300), respectively (Fig. 6c and d). In particular, the fragment ions of *m/z* 118 and 269 (Fig. 6c) versus *m/z* 121 and 266 (Fig. 6d) strongly indicated the different positions of linkages 2-*O*-Me and 3-*O*-Me. The alditol acetate and perdeuteromethyl alditol acetate derivatives in GPL 7-orfAB were detected with the same patterns of 4*N*-acyl-4,6-dideoxy-3-*O*-Me-Hex and 4-*O*-Me-Rha. According to these results, all OSE structures in GPLs derived from three serotype 7 transfor-

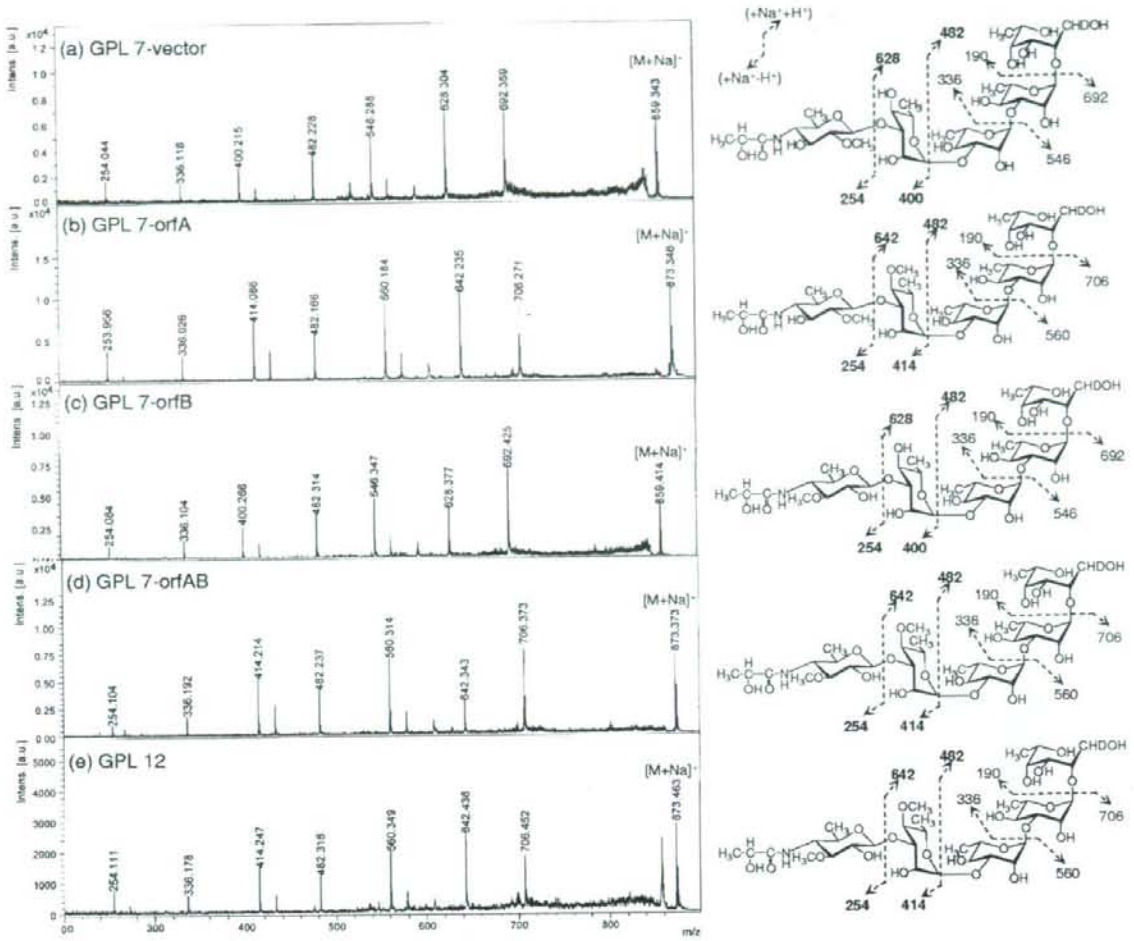

FIG. 5. Fragment patterns of MALDI-TOF/TOF MS spectra of OSEs in GPLs derived from *M. intracellulare* serotype 7, serotype 12, and serotype 7 transformants. The MALDI-TOF/TOF MS spectra were acquired using 10 mg/ml 2,5-dihydroxybenzoic acid in ethanol-water (3:7 [vol/vol]) as the matrix; the molecularly related ions were detected as $[M + Na]^+$ in lift-lift mode. The assigned fragment patterns of glycosyl residues are depicted. a.u., absorbance units.

mants were assigned as listed in Table 2. Altogether, the functions of the two genes were defined. The *orfA* product transfers a methyl group to the C-4 position of Rha next to the terminal sugar, and the *orfB* product transfers a methyl group to the C-3 position of the terminal sugar (Fig. 7). The results demonstrated that GPL 7 in the serotype 7 strain was changed completely to GPL 12 by introduction of the *orfA-orfB* gene cluster.

DISCUSSION

Nontuberculous mycobacteria, including the pathogenic species belonging to the MAC, have serotype-specific GPLs that are important components of the outer layer of the lipid-rich cell walls (5). Structural analyses of some serotype-specific GPLs derived from predominant clinical isolates have been reported (20). We recently determined the complete structure of serotype 7 GPL and the nucleotide sequence of the serotype 7-specific GPL biosynthesis cluster (10). In this cluster, Orfs 1, 3, and 9 might engender transfer of the two molecules of L-Rha and the terminal Hex of serotype 7 GPL (10). Orfs 4, 5, 7, and 8 are homologous to an aminotransferase, a carbamoyl phosphate synthase protein, a metallophosphoesterase, and an acyltransferase, respectively, and possibly relate to the biosynthesis of 2′-hydroxypropanoylamido in the terminal Hex. Based on analysis of sequence homology, these ORFs are probably responsible for the glycosylation of serotype 7 GPL. Serotype 12 GPL has a similar structure to that of serotype 7 GPL, except for O methylation (Fig. 1). In the present study, we cloned the serotype 12 GPL biosynthesis cluster and analyzed its sequence. Although the genetic organization of the *gtfB*-to-*drrC*

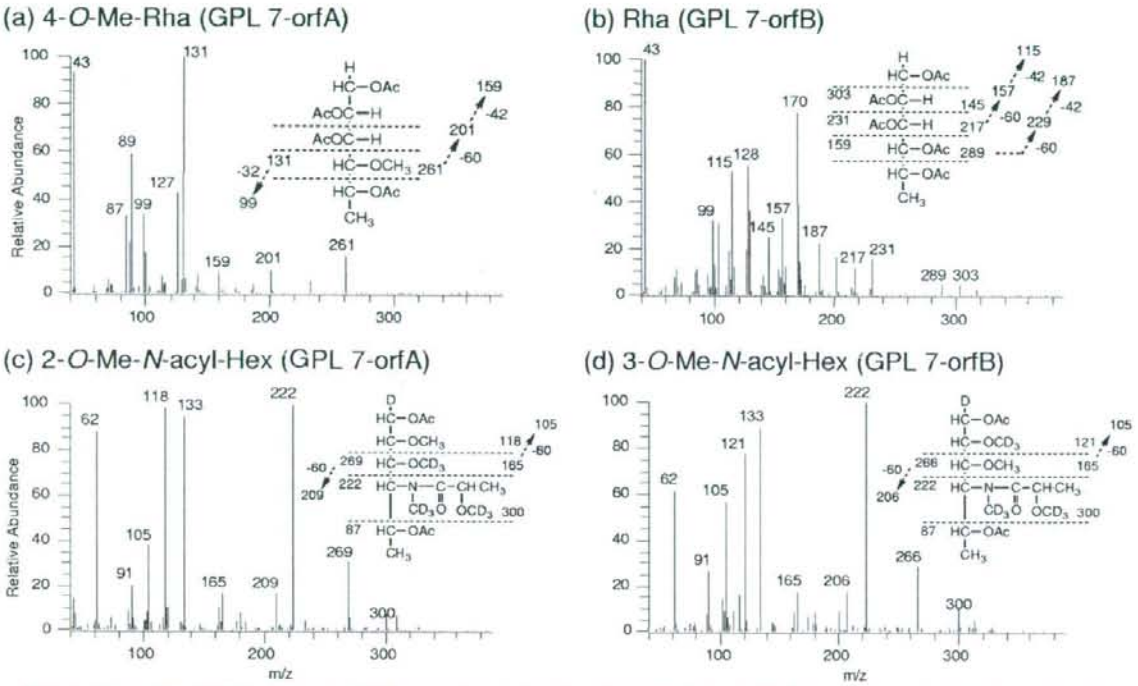

FIG. 6. Preparative GC-MS spectra of alditol acetate (a and b) and perdeuteromethylated alditol acetate (c and d) derivatives. The patterns of prominent fragment ions are presented. An SP-2380 column was used for the analysis of alditol acetate derivatives. The temperature program was started at 60°C, with an increase of 40°C/min to 260°C and a hold at 260°C for 25 min. An Equity-1 column was used for the perdeuteromethylated alditol acetate derivatives. The temperature program was 80°C for 1 min, with an increase of 20°C/min to 180°C followed by an increase of 8°C/min to 280°C.

region of the serotype 12 GPL biosynthetic cluster closely resembled that of serotype 7, significant differences were found in three loci (Fig. 2). The *M. intracellulare* serotype 12 strain NF 103 had one ORF encoding a transposase between *orf7* and *orf8* and had an *orf6* homologous sequence with frameshift inactivation. Orf6 in *M. intracellulare* serotype 7 exhibits sequence similarity to nucleotide sugar epimerases/dehydrogenases, but NF 112, one of the *M. intracellulare* serotype 7 isolates, had an interrupted *orf6* (10). These findings suggest that *orf6* is not involved in biosynthesis of either serotype 7 GPL or serotype 12 GPL. The most important difference between the two serotypes is that *M. intracellulare* serotype 12 had two unique ORFs, *orfA* and *orfB*, instead of *orf2* in *M. intracellulare* serotype 7. Actually, Orf2 in *M. intracellulare* serotype 7 was assigned to a methyltransferase and might be responsible for synthesis of the *O*-methyl group at the C-2 position in the terminal Hex. That possibility suggests that the two unique ORFs for serotype 12 encode *O*-methyltransferases that produce the serotype 12-specific structure. NF 027 (serotype 7) transformed with *orfA* produced 4*N*-acyl-4,6-dideoxy-2-*O*-Me-Hex→4-*O*-Me-Rha→Rha→Rha→6-d-Tal, indicating that the product from *orfA* had activity to synthesize an *O*-methyl group at C-4 in L-Rha next to the terminal Hex (Table 2 and Fig. 7). NF 027 transformed with *orfB* produced 4*N*-acyl-4,6-dideoxy-3-*O*-Me-Hex→Rha→Rha→Rha→6-d-Tal, indicating that the product from *orfB* had activity to synthesize an *O*-methyl group at C-3 in the terminal Hex. NF 027 transformed with *orfA* and *orfB* produced serotype 12-specific GPL,

TABLE 2. Summarized structures of OSEs derived from serotype 7 transformants

GPL	Molecular weight of OSE	Fragment ions in MALDI-TOF/TOF MS	*O*-Methyl group		Structure of OSE
			Terminal sugar	Residue next to terminal sugar	
GPL 7 vector	859	254, 400, 546, 692	2-*O*-Met		4*N*-acyl-4,6-dideoxy-2-*O*-Me-Hex→Rha→Rha→Rha→6-d-Tal
GPL 7-orfA	873	254, 414, 560, 706	2-*O*-Met	4-*O*-Met	4*N*-acyl-4,6-dideoxy-2-*O*-Me-Hex→4-*O*-Me-Rha→Rha→Rha→6-d-Tal
GPL 7-orfB	859	254, 400, 546, 692	3-*O*-Met		4*N*-acyl-4,6-dideoxy-3-*O*-Me-Hex→Rha→Rha→Rha→6-d-Tal
GPL 7-orfAB	873	254, 414, 560, 706	3-*O*-Met	4-*O*-Met	4*N*-acyl-4,6-dideoxy-3-*O*-Me-Hex→4-*O*-Me-Rha→Rha→Rha→6-d-Tal

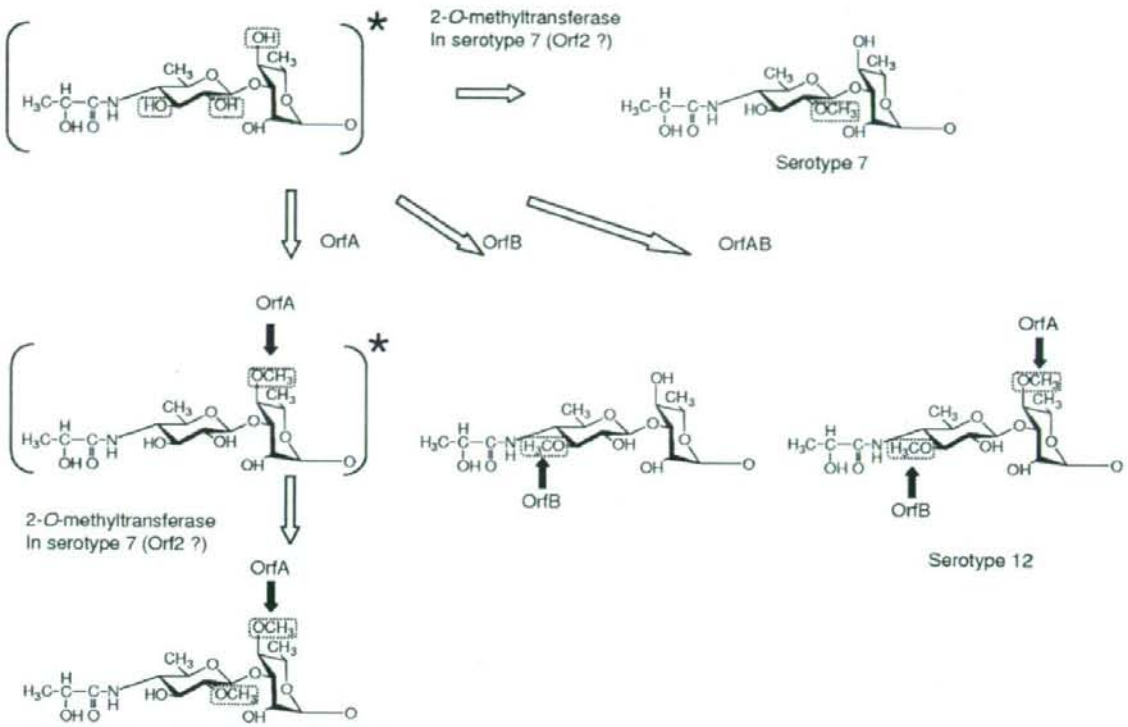

FIG. 7. Synthesis of *O*-methyl groups specific for GPL 7 and GPL 12 in the terminal disaccharide. The structures asterisked in the figure were not detected in this study. Serotype 12-specific O methylations and ORFs responsible for their syntheses are indicated by black arrows.

indicating that these two ORFs were responsible for producing the serotype 12-specific structure. The TLC patterns showed that the migration of GPL 7-orfB was different from that of GPL 7, although the MS data showed that they had the same molecular weight and the same number of methyl groups. A possible explanation for this is that a difference in the position of O methylation could influence hydrogen bond formation and the polarity of the whole molecule and consequently result in a different TLC migration pattern. GPL 7-orfB had an *O*-methyl group at C-3 but not at C-2 in the terminal Hex, indicating that the reaction of O methylation at C-2 by the 2-*O*-methyltransferase in serotype 7 is strongly inhibited by *O*-methylation at C-3. In addition, NF 027 transformed with *orfA* produced a trace of serotype 7-specifc GPL (Fig. 3, lane 4), and NF 027 transformed with *orfA* and *orfB* produced only serotype 12 GPL (Fig. 3, lane 6), suggesting that O methylation at C-2 in the terminal Hex might hinder the reaction of O methylation at C-4 in Rha next to the terminal Hex or that O methylation at C-3 in the terminal Hex might promote the reaction of O methylation at C-4 in Rha.

Because it is not likely that *M. intracellulare* serotypes 7 and 12 independently acquired different methyltransferase genes in the same genetic location between *orf1* and *orf3*, the common ancestor for these two serotypes possibly had all three genes and activated them as the occasion demanded. However, our results showed that reactions of O methylation at C-3 and C-2 in the terminal Hex were competitive (Fig. 3, lane 5, and Table 2). Tsang et al. (26) reported that the frequency of isolation of MAC organisms from AIDS or non-AIDS patients varied among serotypes and that *M. intracellulare* serotype 12 was isolated more often than serotype 7. These two serotypes of *M. intracellulare* might have evolved to adapt to certain environments by losing *orf2* or *orfA-orfB*.

Actually, GPLs are among the immunogenic molecules of the MAC. Tassel et al. reported that the core GPL seems to play a role in suppression of a mitogen-induced blastogenic response of spleen cells (25); furthermore, our previous study showed that sera of patients with MAC disease contain antibodies against GPLs and that the antibody level reflects disease activity (17). In addition, the immunomodulating activity of GPLs on macrophage functions is serotype dependent (13, 24). Elucidation of the structure-activity relationship of GPLs is necessary to better understand the pathogenesis of MAC infection.

ACKNOWLEDGMENTS

This work was supported by grants from the Ministry of Health, Labor and Welfare (Emerging and Re-Emerging Infectious Diseases), the Ministry of Education, Culture, Sports, Science and Technology of Japan, and the Japan Health Sciences Foundation.

N.N. is grateful to M. Kai and M. Makino for helpful discussions.

REFERENCES

1. **Aspinall, G. O., D. Chatterjee, and P. J. Brennan.** 1995. The variable surface glycolipids of mycobacteria: structures, synthesis of epitopes, and biological properties. Adv. Carbohydr. Chem. Biochem. **51:**169–242.
2. **Barrow, W. W., T. L. Davis, E. L. Wright, V. Labrousse, M. Bachelet, and N. Rastogi.** 1995. Immunomodulatory spectrum of lipids associated with *Mycobacterium avium* serovar 8. Infect. Immun. **63:**126–133.
3. **Bhatt, A., N. Fujiwara, K. Bhatt, S. S. Gurcha, L. Kremer, B. Chen, J. Chan, S. A. Porcelli, K. Kobayashi, G. S. Besra, and W. R. Jacobs.** 2007. Deletion of *kasB* in *Mycobacterium tuberculosis* causes loss of acid-fastness and subclinical latent tuberculosis in immunocompetent mice. Proc. Natl. Acad. Sci. USA **104:**5157–5162.
4. **Brennan, P. J., and M. B. Goren.** 1979. Structural studies on the type-specific antigens and lipids of the *Mycobacterium avium-Mycobacterium intracellulare-Mycobacterium scrofulaceum* serocomplex. *Mycobacterium intracellulare* serotype 9. J. Biol. Chem. **254:**4205–4211.
5. **Brennan, P. J., and H. Nikaido.** 1995. The envelope of mycobacteria. Annu. Rev. Biochem. **64:**29–63.
6. **Chatterjee, D., G. O. Aspinall, and P. J. Brennan.** 1987. The presence of novel glucuronic acid-containing, type-specific glycolipid antigens within *Mycobacterium spp*. Revision of earlier structures. J. Biol. Chem. **262:**3528–3533.
7. **Chatterjee, D., and K. H. Khoo.** 2001. The surface glycopeptidolipids of mycobacteria: structures and biological properties. Cell. Mol. Life Sci. **58:** 2018–2042.
8. **Eckstein, T. M., J. T. Belisle, and J. M. Inamine.** 2003. Proposed pathway for the biosynthesis of serovar-specific glycopeptidolipids in *Mycobacterium avium* serovar 2. Microbiology **149:**2797–2807.
9. **Falkinham, J. O.** 1996. Epidemiology of infection by nontuberculous mycobacteria. Clin. Microbiol. Rev. **9:**177–215.
10. **Fujiwara, N., N. Nakata, S. Maeda, T. Naka, M. Doe, I. Yano, and K. Kobayashi.** 2007. Structural characterization of a specific glycopeptidolipid containing a novel *N*-acyl-deoxy sugar from *Mycobacterium intracellulare* serotype 7 and genetic analysis of its glycosylation pathway. J. Bacteriol. **189:**1099–1108.
11. **Hakomori, S.** 1964. A rapid permethylation of glycolipid, and polysaccharide catalyzed by methylsulfinyl carbanion in dimethyl sulfoxide. J. Biochem. (Tokyo) **55:**205–208.
12. **Heidelberg, T., and O. R. Martin.** 2004. Synthesis of the glycopeptidolipid of *Mycobacterium avium* serovar 4: first example of a fully synthetic C-mycoside GPL. J. Org. Chem. **69:**2290–2301.
13. **Kano, H., T. Doi, Y. Fujita, H. Takimoto, I. Yano, and Y. Kumazawa.** 2005. Serotype-specific modulation of human monocyte functions by glycopeptidolipid (GPL) isolated from *Mycobacterium avium* complex. Biol. Pharm. Bull. **28:**335–339.
14. **Kaufmann, S. H.** 2001. How can immunology contribute to the control of tuberculosis? Nat. Rev. Immunol. **1:**20–30.
15. **Khoo, K. H., D. Chatterjee, A. Dell, H. R. Morris, P. J. Brennan, and P. Draper.** 1996. Novel O-methylated terminal glucuronic acid characterizes the polar glycopeptidolipids of *Mycobacterium habana* strain TMC 5135. J. Biol. Chem. **271:**12333–12342.
16. **Khoo, K. H., E. Jarboe, A. Barker, J. Torrelles, C. W. Kuo, and D. Chatterjee.** 1999. Altered expression profile of the surface glycopeptidolipids in drug-resistant clinical isolates of *Mycobacterium avium* complex. J. Biol. Chem. **274:**9778–9785.
17. **Kitada, S., R. Maekura, N. Toyoshima, N. Fujiwara, I. Yano, T. Ogura, M. Ito, and K. Kobayashi.** 2002. Serodiagnosis of pulmonary disease due to *Mycobacterium avium* complex with an enzyme immunoassay that uses a mixture of glycopeptidolipid antigens. Clin. Infect. Dis. **35:**1328–1335.
18. **Krzywinska, E., S. Bhatnagar, L. Sweet, D. Chatterjee, and J. S. Schorey.** 2005. *Mycobacterium avium* 104 deleted of the methyltransferase D gene by allelic replacement lacks serotype-specific glycopeptidolipids and shows attenuated virulence in mice. Mol. Microbiol. **56:**1262–1273.
19. **Maslow, J. N., V. R. Irani, S. H. Lee, T. M. Eckstein, J. M. Inamine, and J. T. Belisle.** 2003. Biosynthetic specificity of the rhamnosyltransferase gene of *Mycobacterium avium* serovar 2 as determined by allelic exchange mutagenesis. Microbiology **149:**3193–3202.
20. **McNeil, M., A. Y. Tsang, and P. J. Brennan.** 1987. Structure and antigenicity of the specific oligosaccharide hapten from the glycopeptidolipid antigen of *Mycobacterium avium* serotype 4, the dominant mycobacterium isolated from patients with acquired immune deficiency syndrome. J. Biol. Chem. **262:** 2630–2635.
21. **Miyamoto, Y., T. Mukai, N. Nakata, Y. Maeda, M. Kai, T. Naka, I. Yano, and M. Makino.** 2006. Identification and characterization of the genes involved in glycosylation pathways of mycobacterial glycopeptidolipid biosynthesis. J. Bacteriol. **188:**86–95.
22. **Porcelli, S. A., and R. L. Modlin.** 1999. The CD1 system: antigen-presenting molecules for T cell recognition of lipids and glycolipids. Annu. Rev. Immunol. **17:**297–329.
23. **Smith, I.** 2003. *Mycobacterium tuberculosis* pathogenesis and molecular determinants of virulence. Clin. Microbiol. Rev. **16:**463–496.
24. **Takegaki, Y.** 2000. Effect of serotype specific glycopeptidolipid (GPL) isolated from *Mycobacterium avium* complex (MAC) on phagocytosis and phagosome-lysosome fusion of human peripheral blood monocytes. Kekkaku **75:**9–18.
25. **Tassell, S. K., M. Pourshafie, E. L. Wright, M. G. Richmond, and W. W. Barrow.** 1992. Modified lymphocyte response to mitogens induced by the lipopeptide fragment derived from *Mycobacterium avium* serovar-specific glycopeptidolipids. Infect. Immun. **60:**706–711.
26. **Tsang, A. Y., J. C. Denner, P. J. Brennan, and J. K. McClatchy.** 1992. Clinical and epidemiological importance of typing of *Mycobacterium avium* complex isolates. J. Clin. Microbiol. **30:**479–484.

JOURNAL OF BACTERIOLOGY, May 2008, p. 3613–3621 Vol. 190, No. 10
0021-9193/08/$08.00+0 doi:10.1128/JB.01850-07

Structural Analysis and Biosynthesis Gene Cluster of an Antigenic Glycopeptidolipid from *Mycobacterium intracellulare*▽†

Nagatoshi Fujiwara,[1]* Noboru Nakata,[2] Takashi Naka,[1,3] Ikuya Yano,[3] Matsumi Doe,[4] Delphi Chatterjee,[5] Michael McNeil,[5] Patrick J. Brennan,[5] Kazuo Kobayashi,[6] Masahiko Makino,[2] Sohkichi Matsumoto,[1] Hisashi Ogura,[7] and Shinji Maeda[8]

Department of Host Defense[1] and Virology,[7] Osaka City University Graduate School of Medicine, Osaka 545-8585, Japan; Department of Microbiology, Leprosy Research Center, National Institute of Infectious Diseases, Tokyo 189-0002, Japan[2]; Japan BCG Laboratory, Tokyo 204-0022, Japan[3]; Department of Chemistry, Graduate School of Science, Osaka City University, Osaka 558-8585, Japan[4]; Department of Microbiology, Immunology and Pathology, Colorado State University, Colorado 80523[5]; Department of Immunology, National Institute of Infectious Diseases, Tokyo 162-8640, Japan[6]; and Molecular Epidemiology Division, Mycobacterium Reference Center, The Research Institute of Tuberculosis, Japan Anti-Tuberculosis Association, Tokyo 204-8533, Japan[8]

Received 24 November 2007/Accepted 1 March 2008

***Mycobacterium avium-Mycobacterium intracellulare* complex (MAC) is the most common isolate of nontuberculous mycobacteria and causes pulmonary and extrapulmonary diseases. MAC species can be grouped into 31 serotypes by the epitopic oligosaccharide structure of the species-specific glycopeptidolipid (GPL) antigen. The GPL consists of a serotype-common fatty acyl peptide core with 3,4-di-*O*-methyl-rhamnose at the terminal alaninol and a 6-deoxy-talose at the *allo*-threonine and serotype-specific oligosaccharides extending from the 6-deoxy-talose. Although the complete structures of 15 serotype-specific GPLs have been defined, the serotype 16-specific GPL structure has not yet been elucidated. In this study, the chemical structure of the serotype 16 GPL derived from *M. intracellulare* was determined by using chromatography, mass spectrometry, and nuclear magnetic resonance analyses. The result indicates that the terminal carbohydrate epitope of the oligosaccharide is a novel *N*-acyl-dideoxy-hexose. By the combined linkage analysis, the oligosaccharide structure of serotype 16 GPL was determined to be 3-2′-methyl-3′-hydroxy-4′-methoxy-pentanoyl-amido-3,6-dideoxy-β-hexose-(1→3)-4-*O*-methyl-α-L-rhamnose-(1→3)-α-L-rhamnose-(1→3)-α-L-rhamnose-(1→2)-6-deoxy-α-L-talose. Next, the 22.9-kb serotype 16-specific gene cluster involved in the glycosylation of oligosaccharide was isolated and sequenced. The cluster contained 17 open reading frames (ORFs). Based on the similarity of the deduced amino acid sequences, it was assumed that the ORF functions include encoding three glycosyltransferases, an acyltransferase, an aminotransferase, and a methyltransferase. An *M. avium* serotype 1 strain was transformed with cosmid clone no. 253 containing *gtfB-drrC* of *M. intracellulare* serotype 16, and the transformant produced serotype 16 GPL. Together, the ORFs of this serotype 16-specific gene cluster are responsible for the biosynthesis of serotype 16 GPL.**

Mycobacterial diseases, such as tuberculosis and infection due to nontuberculous mycobacteria (NTM), are still among the most serious infectious diseases in the world. The incidence is increasing because of the spread of drug-resistant mycobacteria and the human immunodeficiency virus (HIV) infection/AIDS epidemic (16, 17, 30). *Mycobacterium avium-Mycobacterium intracellulare* complex (MAC) is the most common among isolates of NTM and is distributed ubiquitously in the environment. MAC causes pulmonary and extrapulmonary diseases in both immunocompromised and immunocompetent hosts. It affects primarily patients with advanced HIV infection. MAC includes at least two mycobacterial species, *M. avium* and *M. intracellulare*, that cannot be differentiated on the basis of traditional physical and biochemical tests (1, 41).

The cell envelope of mycobacteria is a complex and unusual structure. The key feature of this structure is an extraordinarily high lipid concentration (6, 10). To better understand the pathogenesis of MAC infection, it is necessary to elucidate the molecular structure and biochemical features of the lipid components. Among MAC lipids, the glycopeptidolipid (GPL) is of particular importance, because it shows not only serotype-specific antigenicity but also immunomodulatory activities in the host immune responses (2, 9, 23). Structurally, GPLs are composed of two parts, a tetrapeptide-amino alcohol core and a variable oligosaccharide (OSE). C_{26}-C_{34} fatty acyl-D-phenylalanine-D-*allo*-threonine-D-alanine-L-alaninol (D-Phe-D-*allo*-Thr-D-Ala-L-alaninol) is further linked with 6-deoxy talose (6-d-Tal) and 3,4-di-*O*-methyl rhamnose (3,4-di-*O*-Me-Rha) at D-*allo*-Thr and the terminal L-alaninol, respectively. This type of core GPL is found in all subspecies of MAC, shows a common antigenicity, and is further glycosylated at 6-d-Tal to form a serotype-specific OSE.

At present, 31 distinct serotype-specific GPLs have been identified serologically and chromatographically (9). Although the standard technique for differentiation of MAC subspecies

* Corresponding author. Mailing address: Department of Host Defense, Osaka City University Graduate School of Medicine, 1-4-3 Asahi-machi, Abeno-ku, Osaka 545-8585, Japan. Phone: 81 6 6645 3746. Fax: 81 6 6645 3747. E-mail: fujiwara@med.osaka-cu.ac.jp.

† Supplemental material for this article may be found at http://jb.asm.org/.

▽ Published ahead of print on 7 March 2008.

has been serotyping based on the OSE residue of its GPL, the complete structures of only 15 GPLs have been defined. In addition to the chemical structures of various GPLs, genes encoding the glycosylation pathways in the biosynthesis of GPL have been identified and characterized (12, 21, 31). Epidemiological studies have shown that MAC serotypes 4 and 8 are the most frequently isolated from patients, and MAC serotype 16 is one of the next most common groups (32, 40). It has been suggested that the serotypes of MAC isolates participate in their virulence (29), and thus, understanding of the structure-pathogenicity relationship of GPLs is necessary. In the present study, we demonstrate the complete OSE structure of the GPL derived from serotype 16 MAC (*M. intracellulare*), which has a unique terminal-acylated-amido sugar, and we characterized the serotype 16 GPL-specific gene cluster involved in the glycosylation of carbohydrates.

MATERIALS AND METHODS

Bacterial strains and preparation of GPL. *M. intracellulare* serotype 16 strain ATCC 13950^T (NF 115) was purchased from the American Type Culture Collection (Manassas, VA). Three clinical isolates of *M. intracellulare* serotype 16 (NF 116 and 117) and *M. avium* serotype 1 (NF 113) were maintained in The Research Institute of Tuberculosis, Japan Anti-Tuberculosis Association. The preparation of GPL was performed as described previously (18, 24, 26). Briefly, each strain of *M. intracellulare* serotype 16 was grown in Middlebrook 7H9 broth (Difco Laboratories, Detroit, MI) with 0.5% glycerol and 10% Middlebrook oleic acid-albumin-dextrose-catalase enrichment (Difco) at 37°C for 2 to 3 weeks. The heat-killed bacteria were sonicated, and crude lipids were extracted with chloroform-methanol (2:1, vol/vol). The extracted lipids were dried and hydrolyzed with 0.2 N sodium hydroxide in methanol at 37°C for 2 h. After neutralization with 6 N hydrochloric acid, alkaline-stable lipids were partitioned by a two-layer system of chloroform-methanol (2:1, vol/vol) and water. The organic phase was recovered, evaporated, and precipitated with acetone to remove any acetone-insoluble components containing phospholipids and glycolipids. The supernatant was collected by centrifugation, dried, and then treated with a Sep-Pak silica cartridge (Waters Corporation, Milford, MA) with washing (chloroform-methanol, 95:5, vol/vol) and elution (chloroform-methanol, 1:1, vol/vol) for partial purification. GPL was completely purified by preparative thin-layer chromatography (TLC) of Silica Gel G (20 by 20 cm, 250 μm; Uniplate; Analtech, Inc., Newark, DE). The TLC plate was repeatedly developed with chloroform-methanol-water (65:25:4 and 60:16:2, vol/vol/vol) until a single spot was obtained. After exposure of the TLC plate to iodine vapor, the GPL band was marked, and then, the silica gels were scraped off and the GPL was eluted with chloroform-methanol (2:1, vol/vol).

Preparation of OSE moiety. β elimination of GPL was performed with alkaline borohydride, and the OSE elongated from D-*allo*-Thr was released as described previously (18, 24). Briefly, the GPL was dissolved in ethanol, and an equal volume of 10 mg/ml sodium borohydride or borodeuteride in 0.5 N sodium hydroxide was added and then stirred at 60°C for 16 h. The reaction mixture was decationized with Dowex 50W-X8 beads (Dow Chemical Company, Midland, MI), collected, and evaporated under nitrogen to remove boric acid. The dried residue was partitioned in two layers of chloroform-methanol (2:1, vol/vol) and water. The upper aqueous phase was recovered and evaporated. In these processes, the serotype 16-specific OSE was purified as an oligoglycosyl alditol.

MALDI-TOF and MALDI-TOF/TOF MS analyses. The molecular species of the intact GPL was detected by matrix-assisted laser desorption ionization–time of flight mass spectrometry (MALDI-TOF MS) with an Ultraflex II (Bruker Daltonics, Billerica, MA). The GPL was dissolved in chloroform-methanol (2:1, vol/vol) at a concentration of 1 mg/ml, and 1 μl was applied directly to the sample plate, and then 1 μl of 10 mg/ml 2,5-dihydroxybenzoic acid in chloroform-methanol (1:1, vol/vol) was added as a matrix. The intact GPL was analyzed in the reflectron mode with an accelerating voltage operating in a positive mode of 20 kV (5). Then the fragment pattern of the OSE was analyzed with MALDI-TOF/TOF MS. The OSE was dissolved in ethanol-water (3:7, vol/vol), and the matrix was 10 mg/ml 2,5-dihydroxybenzoic acid in ethanol-water (3:7, vol/vol). The OSE and the matrix were applied to the sample plate according to the method for intact GPL and analyzed in the lift-lift mode.

GC and GC-MS analyses of carbohydrates and *N*-acylated short-chain fatty acid. To determine the glycosyl composition and linkage position, gas chromatography (GC) and GC-MS analyses of partially methylated alditol acetate derivatives were performed. Perdeuteromethylation was conducted by the modified procedure of Hakomori as described previously (18, 20). Briefly, the dried OSE was dissolved with a mixture of dimethyl sulfoxide and sodium hydroxide, and deuteromethyl iodide was added. The reaction mixture was stirred at room temperature for 15 min and then water and chloroform were added. The chloroform-containing perdeuteromethylated OSE layer was collected, washed with water two times, and then completely evaporated. Partially deuteromethylated alditol acetates were prepared from perdeuteromethylated OSE by hydrolysis with 2 N trifluoroacetic acid at 120°C for 2 h, reduction with 10 mg/ml sodium borodeuteride at 25°C for 2 h, and acetylation with acetic anhydride at 100°C for 1 h (8, 18, 25). To identify amino-linked fatty acids, acidic methanolysis of serotype 16 GPL was performed with 1.25 M hydrogen chloride in methanol (Sigma-Aldrich, St. Louis, MO) at 100°C for 90 min, and the fatty acid methyl esters were extracted with *n*-hexane under the cooled ice. GC was performed using a 5890 series II gas chromatograph (Hewlett Packard, Avondale, PA) equipped with a fused SPB-1 capillary column (30 m, 0.25-mm inner diameter; Supelco Inc., Bellefonte, PA). Helium was used for electron impact (EI)-MS and isobutane for chemical ionization (CI)-MS as a carrier gas. A JMS SX102A double-focusing mass spectrometer (JEOL, Tokyo, Japan) was connected to the gas chromatograph as a mass detector. The molecular separator and the ion source energy were 70 eV for EI and 30 eV for CI, and the accelerating voltage was 8 kV. The D and L configurations of Rha residues were determined by comparative GC-MS analysis of trimethylsilylated (*S*)-(+)-sec-butyl glycosides and (*R*)-(−)-sec-butyl glycosides prepared from an authentic standard L-Rha (19).

NMR analysis of GPL. The GPL was dissolved in chloroform-d ($CDCl_3$)-methanol-d_4 (CD_3OD) (2:1, vol/vol). To define the anomeric configurations of each glycosyl residue, ^1H and ^{13}C nuclear magnetic resonance (NMR) was employed. Both homonuclear correlation spectrometry (COSY) and ^1H-detected [^1H, ^{13}C] heteronuclear multiple-quantum correlation (HMQC) were recorded with a Bruker Avance-600 (Bruker BioSpin Corp., Billerica, MA), as described previously (9, 18, 24, 34).

Construction of *M. intracellulare* serotype 16 cosmid library. A cosmid library of *M. intracellulare* serotype 16 strain ATCC 13950^T was constructed as described previously (18). Bacterial cells were disrupted mechanically, and genomic DNA was extracted with phenol-chloroform and then precipitated with ethanol. Genomic DNA randomly sheared into 30- to 50-kb fragments in the extraction process was fractionated and electroeluted from agarose gels using a Takara Recochip (Takara, Kyoto, Japan). These DNA fragments were rendered blunt ended using T4 DNA polymerase and deoxynucleoside triphosphates and then were ligated to dephosphorylated arms of pYUB412 (XbaI-EcoRV and EcoRV-XbaI), which were the kind gifts of William R. Jacobs, Jr. (Department of Microbiology and Immunology, Albert Einstein College of Medicine, Bronx, NY). The cosmid vector pYUB412 is an *Escherichia coli-Mycobacterium* shuttle vector with the *int-attP* sequence for integration into a mycobacterial chromosome, *oriE* for replication in *E. coli*, a hygromycin resistance gene, and an ampicillin resistance gene. After in vitro packaging using Gigapack III Gold extracts (Stratagene, La Jolla, CA), recombinant cosmids were introduced into *E. coli* STBL2 [F$^-$ *mcrA* Δ(*mcrBC-hsdRMS-mrr*) *recA1 endA1 lon gyrA96 thi supE44 relA1* λ Δ(*lac-proAB*)] and stored at −80°C in 50% glycerol.

Isolation of cosmid clones carrying biosynthesis gene cluster of serotype 16 GPL and sequence analysis. Isolation of DNA from *E. coli* transductants was performed as described by Supply et al., with modifications (39). The colonies were picked, transferred to a 1.5-ml tube containing 50 μl of water, and then heated at 98°C for 5 min. After centrifugation at 14,000 rpm for 5 min, the supernatant was used as the PCR template. PCR was used to isolate cosmid clones carrying the rhamnosyltransferase (*rtfA*) gene with primers rtfA-F (5′-TTTGGAGCGACGAGTTCATC-3′) and rtfA-R (5′-GTGTAGTTGACCACG CCGAC-3′). *rtfA* encodes an enzyme responsible for the transfer of Rha to 6-d-Tal in OSE (14, 31). The insert of cosmid clone no. 253 was sequenced using a BigDye Terminator, version 3.1, cycle sequencing kit (Applied Biosystems, Foster City, CA) and an ABI Prism 310 gene analyzer (Applied Biosystems). The putative function of each open reading frame (ORF) was identified by similarity searches between the deduced amino acid sequences and known proteins using BLAST (http://www.ncbi.nlm.nih.gov/BLAST/) and FramePlot (http://www.nih.go.jp/~jun/cgi-bin/frameplot.pl) with the DNASIS computer program (Hitachi Software Engineering, Yokohama, Japan).

Transformation of *M. avium* serotype 1 strain with cosmid clone no. 253. An *M. avium* serotype 1 strain (NF113) was transformed with pYUB412-cosmid clone no. 253 by electroporation, and hygromycin-resistant colonies were iso-

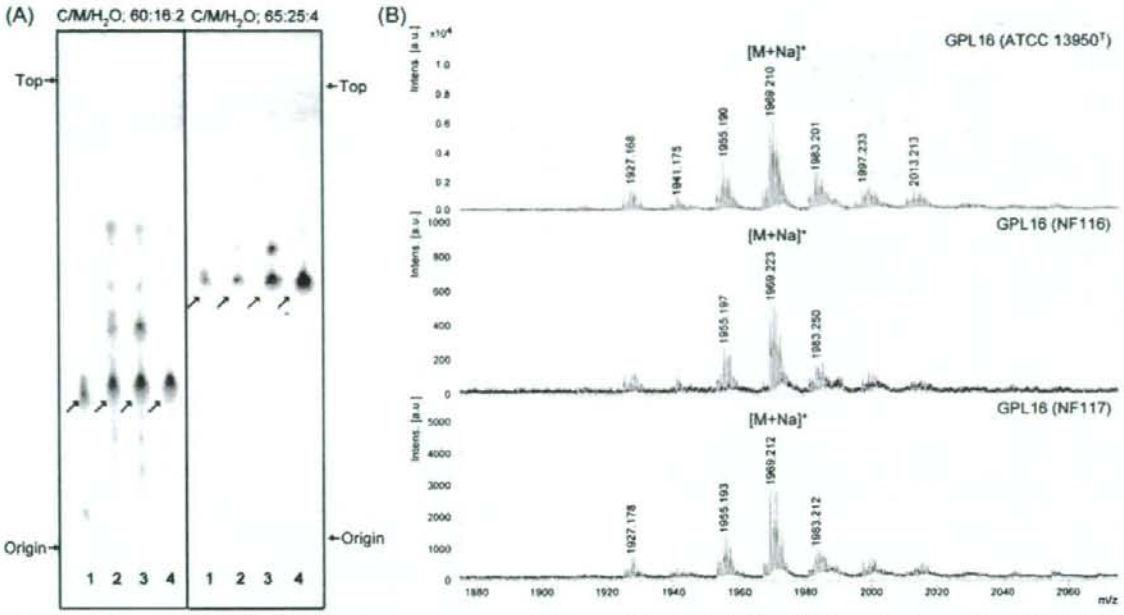

FIG. 1. TLC patterns and MALDI-TOF MS spectra of serotype 16 GPL. (A) Serotype 16 GPL purified from *M. intracellulare* ATCC 13950^T (NF 115) and the alkaline-stable lipids derived from ATCC 13950^T and two clinical isolates (NF 116 and 117) from left to right were developed on TLC plates with solvent systems of chloroform-methanol-water (65:25:4 and 60:16:2, vol/vol/vol). (B) The MALDI-TOF MS spectra were acquired using 10 mg/ml 2,5-dihydroxybenzoic acid in chloroform-methanol (1:1, vol/vol) as a matrix, and the molecularly related ions were detected as $[M+Na]^+$ in positive mode. Intens., intensity; a.u., absorbance units.

lated. Alkaline-stable lipids were prepared, and productive GPLs were examined by TLC and MALDI-TOF MS analyses.

Nucleotide sequence accession number. The nucleotide sequence reported here has been deposited in the NCBI GenBank database under accession no. AB355138.

RESULTS

Purification and molecular weight of intact GPL. Serotype 16 GPL from *M. intracellulare* ATCC 13950^T (NF 115) was detected as a spot by TLC, and the R_f values were 0.35 and 0.56 when developed with chloroform-methanol-water (60:16:2 and 65:25:4, vol/vol/vol, respectively). Two clinical isolates of *M. intracellulare*, NF 116 and 117, had serotype 16 GPLs that showed the same R_f values as the serotype 16 GPL derived from strain ATCC 13950^T. The serotype 16 GPL of *M. intracellulare* strain ATCC 13950^T was purified repeatedly by TLC and was shown as a single spot by TLC (Fig. 1A). The MALDI-TOF MS spectra of each serotype 16 GPL showed *m/z* 1969 for $[M+Na]^+$ as the main molecularly related ion in positive mode, with the homologous ions differing by 14 mass units at 1,955 and 1,983 (Fig. 1B). As a result, the main molecular weight of serotype 16 GPL was 1,946, which implied that it has a novel carbohydrate chain elongated from D-*allo*-Thr.

Carbohydrate composition of serotype 16 OSE. To determine the glycosyl compositions of serotype 16 OSE, alditol acetate derivatives of the serotype 16 GPL were analyzed by GC and GC-MS. The structurally defined serotype 4 GPL was used as a reference standard (9, 35). Comparison of the retention time and GC mass spectra (Fig. 2) with the alditol acetate derivatives of the serotype 16 GPL showed the presence of 3,4-di-*O*-Me-Rha, 4-*O*-Me-Rha, Rha, 6-d-Tal, and an unknown sugar residue (X1) in a ratio of approximately 1:1:2:1:1. The alditol acetate of X1 was eluted at a retention time of 29.3 min, greater than that of glucitol acetate on the SPB-1 column. The CI-MS spectrum of X1 was $[M+H]^+$ at *m/z* 520 as a parent ion and *m/z* 460 as a loss of 60 (acetate). The fragment ions of X1 sugar showed characteristic patterns in EI-MS. *m/z* 360 indicated the cleavage of C-3 and C-4, and *m/z* 300, 240, and 180 were fragmented with a loss of 60 (acetate). Similarly, *m/z* 374 indicated the cleavage of C-2 and C-3, and *m/z* 314 and 254 were fragmented with a loss of 60 (Fig. 3A and B). These results indicated that X1 was 3,6-dideoxy hexose (Hex). The odd molecular weight of X1, 519, and *m/z* 187, 127, and 59 implied the presence of one amido group esterified with a short-chain fatty acid, possibly. After methanolysis of serotype 16 GPL, the resultant fatty acid methyl esters were extracted carefully and analyzed by GC-MS. The EI-MS spectrum of a short-chain fatty acid methyl ester showed mass ions at *m/z* 176 ($[M]^+$), 145 ($[M-31]^+$), 117 ($[M-59]^+$), 99, 88, 85, and 59 (Fig. 3C) (33, 37). Taking the results together, X1 was structurally determined to be 3-2′-methyl-3′-hydroxy-4′-methoxy-pentanoyl-amido-3,6-dideoxy-Hex.

Glycosyl linkage and sequence of serotype 16 OSE. To determine the glycosyl linkage and sequence of the OSE, GC-MS of perdeuteromethylated alditol acetates and MALDI-TOF/TOF MS of the oligoglycosyl alditol from serotype 16 OSE

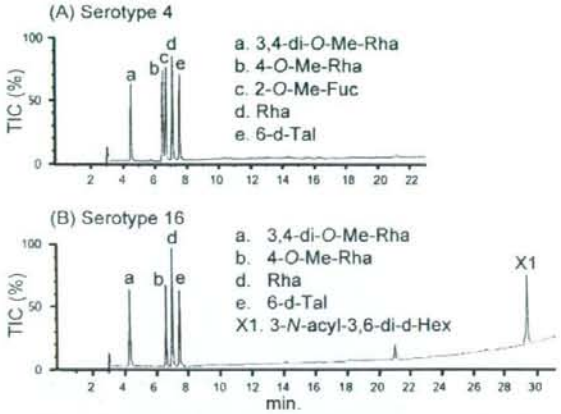

FIG. 2. Gas chromatograms of the alditol acetate derivatives from serotype 4 (A) and serotype 16 (B) GPLs. Total ion chromatograms (TIC) are shown. GC was performed on an SPB-1-fused silica column with a temperature program of 160°C for 2 min, followed by an increase of 4°C/min to 220°C, and holding at 220°C for 15 min. Comparison to the GC spectrum of serotype 4 GPL shows that serotype 16 GPL is composed of 3,4-di-*O*-Me-Rha, 4-*O*-Me-Rha, Rha, 6-d-Tal, and an unknown X1 sugar residue.

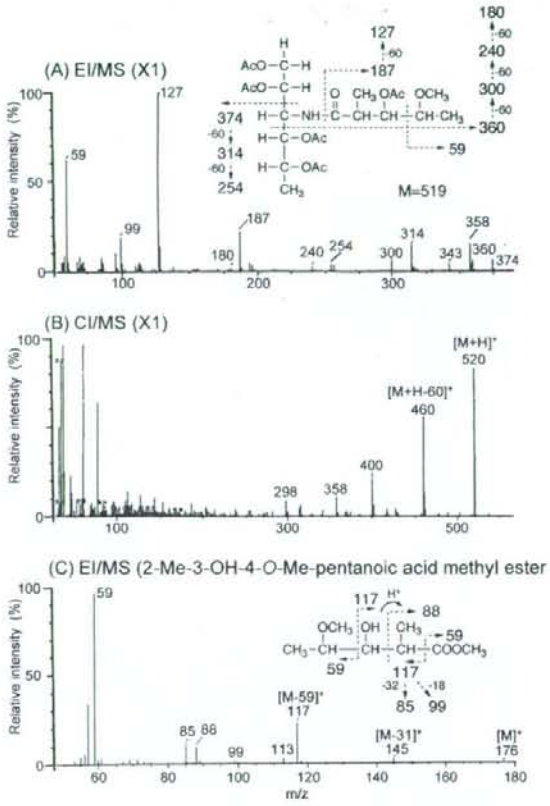

FIG. 3. EI-MS and CI-MS spectra of the alditol acetate derivative from X1 (A and B) and *N*-acylated-short-chain fatty acid methyl ester (C). The pattern of prominent fragment ions is illustrated. The CG column and condition were described in the legend for Fig. 2.

were performed. As shown in Fig. 4, the GC-MS spectra of perdeuteromethylated alditol acetates were assigned four major peaks, 1,3,4,5-tetra-*O*-deuteromethyl-2-*O*-acetyl-6-deoxytalitol (*m/z* 109, 132, 154, 167, and 214); 2,4-di-*O*-deuteromethyl-1,3,5-tri-*O*-acetyl-rhamnitol (*m/z* 121, 134, 205, 240, and 253); 2-*O*-deuteromethyl-4-*O*-methyl-1,3,5-tri-*O*-acetyl-rhamnitol (*m/z* 121, 131, 202, and 237); and 2,4-di-*O*-deuteromethyl-1,5-di-*O*-acetyl-3-2′-methyl-3′-*O*-deuteromethyl-4′methoxypentanoyl-deuteromethylamido-3,6-dideoxy-hexitol (*m/z* 121, 134, and 341). These results revealed that the 6-d-Tal residue was linked at C-2; Rha and 4-*O*-Me-Rha were linked at C-1 and C-3; and the nonreducing terminus, 3-2′-methyl-3′-hydroxy-4′-methoxy-pentanoyl-amido-3,6-dideoxy-Hex, was C-1 linked. The MALDI-TOF/TOF MS spectrum of the oligoglycosyl alditol from serotype 16 OSE afforded the expected molecular ions $[M+Na]^+$ at *m/z* 931, together with the characteristic mass increments in the series of glycosyloxonium ions formed on fragmentation at *m/z* 312, 472, 618, and 764 from the terminal sugar *N*-acyl-Hex to 6-d-Tal and at *m/z* 336, 482, and 642 from 6-d-Tal to *N*-acyl-Hex (Fig. 5). Rha residues were determined to be in the L absolute configuration by comparative GC-MS analyses of trimethylsilylated (*S*)-(+)-sec-butyl glycosides and (*R*)-(−)-sec-butylglycosides (see Fig. S1 in the supplemental material). Taken together, these results established the sequence and linkage arrangement 3-2′-methyl-3′-hydroxy-4′-methoxy-pentanoyl-amido-3,6-dideoxy-Hex-(1→3)-4-*O*-Me-Rha-(1→3)-L-Rha-(1→3)-L-Rha-(1→2)-6-d-Tal, exclusively.

NMR analysis of serotype 16 OSE. The ^{1}H NMR and ^{1}H-^{1}H COSY analyses of the serotype 16 GPL revealed six distinct anomeric protons with corresponding H1-H2 cross peaks in the low field region at δ4.93, 4.92, 4.92, 4.84, 4.65 ($J_{1\text{-}2}$ = 2 to 3 Hz, indicative of α-anomers) and 4.51 (a doublet, $J_{1\text{-}2}$ = 7.7 Hz, indicative of a β-hexosyl unit). When further analyzed by ^{1}H-detected [^{1}H, ^{13}C] two-dimensional HMQC, the anomeric protons resonating at δ4.93, 4.92, 4.92, 4.84, 4.65, and 4.51 have C-1s resonating at δ101.57, 95.73, 101.40, 102.56, 100.97, and 103.36, respectively (for a summary, see Table S1 in the supplemental material). The J_{CH} values for each of these protons were calculated to be 171, 170, 171, 170, 169, and 161 Hz by measurement of the inverse-detection nondecoupled two-dimensional HMQC (Fig. 6). These results established that the terminal amido-Hex was a β configuration and the others were α-anomers.

Cloning and sequence of serotype 16 GPL biosynthesis cluster. To isolate the serotype 16 GPL biosynthesis cluster, the genomic cosmid library of *M. intracellulare* serotype 16 strain ATCC 13950^T was constructed. Primers were designed to amplify the region corresponding to the *rtfA* gene. More than 300 cosmid clones were tested using colony PCR with *rtfA* primers, and the positive clones no. 51 and 253 were isolated from the *E. coli* transductants. PCR analysis revealed that clone no. 253 contained a *drrC* gene but that clone no. 51 did not. Thus, we used clone no. 253 for subsequent sequence analysis for the *gtfB-drrC* region. The 22.9-kb region of *M. intracellulare* sero-

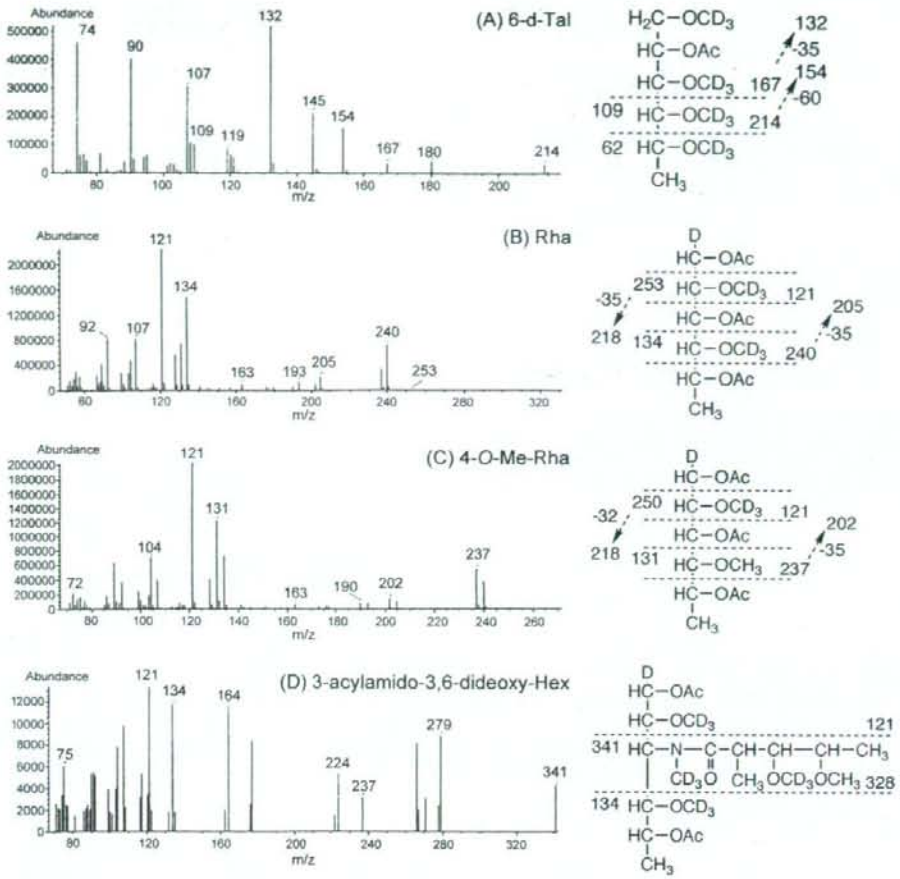

FIG. 4. GC-MS spectra of individual perdeuteromethylated alditol acetate derivatives from serotype 16 OSE. The formation of prominent fragment ions is illustrated; fragments were assigned to 1,3,4,5-tetra-*O*-deuteromethyl-2-*O*-acetyl-6-deoxy-talitol (A), 2,4-di-*O*-deuteromethyl-1,3,5-tri-*O*-acetyl-rhamnitol (B), 2-*O*-deuteromethyl-4-*O*-methyl-1,3,5-tri-*O*-acetyl-rhamnitol (C), and 2,4-di-*O*-deuteromethyl-1,5-di-*O*-acetyl-3-2′-methyl-3′-*O*-deuteromethyl-4′-methoxy-pentanoyl-deuteromethylamido-3,6-dideoxy-hexitol (D).

type 16 ATCC 13950^T was deposited in the NCBI GenBank database (accession no. AB355138). The similarity to protein sequences of each ORF is summarized in Table 1, and the genetic map for the serotype 16 GPL biosynthetic cluster was compared with those of serotype 2, 4, and 7 GPLs (Fig. 7). The *gtfB* and *drrC* genes of *M. intracellulare* serotype 16 ATCC 13950^T had 99.8% and 83.7% DNA identities with those of *M. intracellulare* serotype 7 ATCC 35847, respectively. In the DNA region between *gtfB* and *drrC* (20.8 kb), 17 ORFs were observed. Four ORFs (ORF 1, 2, 16, and 17) were homologous to those found in the same region of serotype 7-specific DNA, and the others were unique to the serotype 16 strain. No insertion of insertion elements or transposons was detected in this region. The nucleotide sequences of the ORF 1 and ORF 2 in serotype 16 strain ATCC 13950^T were homologous to those of ORF 1 and ORF 8 in serotype 7, respectively, suggesting that these two ORFs have the same function. The similarity of the deduced amino acid sequences suggested the possibility that the functions of ORF 3 and ORF 6 are to encode methyltransferase and aminotransferase, respectively. The deduced amino acid sequences of ORF 4 and ORF 5 showed significant similarities to the WxcM protein, the function of which is not clear. Interestingly, the deduced amino acid sequences of ORF 16 and ORF 17 of serotype 16 were homologous to ORF 9 of serotype 7. ORFs 1, 16, and 17 have considerable homology to glycosyltransferases. Nine ORFs, which are possibly involved in fatty acid synthesis, were detected between ORF 7 and ORF 15. It is notable that ORF 13 had a chimeric structure. The N-terminal half of ORF 13 showed similarity to phosphate butyryl/acetyl transferases, but the C-terminal half showed similarity to short-chain reductase/dehydrogenases. These results suggest that this region of DNA is responsible for the biosynthesis of the serotype 16-specific GPL.

Expression of cosmid clone no. 253 in *M. avium* serotype 1 strain. The OSE of serotype 1 GPL was composed of α-L-Rha-

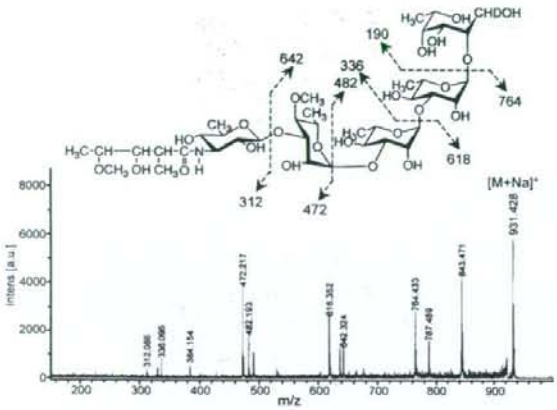

FIG. 5. MALDI-TOF/TOF MS spectrum of serotype 16 OSE. The formation of a characteristic increment in fragment ions is illustrated. The matrix was 10 mg/ml 2,5-dihydroxybenzoic acid in ethanol-water (3:7, vol/vol), and it was performed in the lift-lift mode. Intens., intensity; a.u., absorbance units.

(1→2)-6-d-L-Tal (9). The *M. avium* serotype 1 strain (NF113) was transformed with cosmid clone no. 253 containing a serotype 16-specific gene cluster and produced a new GPL with a different R_f value by TLC compared to serotype 1 GPL (Fig. 8A). The R_f value of the new GPL was identical to that of the serotype 16 GPL. The molecular weight of intact GPL, the fragment pattern of its OSE, and the GC pattern of the alditol acetate derivatives were completely equivalent to those of the serotype 16 GPL (see Fig. S2 in the supplemental material). As a result, the transformant of the serotype 1 strain expressed the cosmid clone no. 253 gene cluster and produced the serotype 16 GPL.

DISCUSSION

MAC species have serotype-specific GPLs that are characteristic components of the outer layer of the cell wall (6, 9). In addition to their serological differentiation, the chemical structures of 15 serotype-specific GPLs derived from the predominant clinical isolates have been analyzed; however, those of other GPLs remain unclear. The present study demonstrates the chemical structure of the serotype 16 GPL derived from *M. intracellulare*. We determined the glycosyl composition, linkage positions, and anomeric and ring configurations of the glycosyl residues of the serotype 16 GPL, and its OSE was defined as 3-2′-methyl-3′-hydroxy-4′-methoxy-pentanoyl-amido-3,6-dideoxy-β-Hex-(1→3)-4-*O*-methyl-α-L-Rha-(1→3)-α-L-Rha-(1→3)-α-L-Rha-(1→2)-6-d-α-L-Tal (Fig. 8B). The serotype 16 GPL should be listed as a group 2 polar GPL in the structural classification of Chatterjee and Khoo (9).

The GPLs of serotypes 7, 12, 17, and 19 have already been classified as group 2 GPLs, which are commonly composed of R→α-L-Rha-(1→3)-α-L-Rha-(1→2)-6-d-L-Tal (R, variable region), possessing a characteristic terminal sugar such as *N*-acyldeoxy-Hex. Indeed, the presence of an amido sugar has been reported in only five GPLs, serotypes 7, 12, 14, 17, and 25 (8, 9, 18). It has been determined that the OSE structure of the

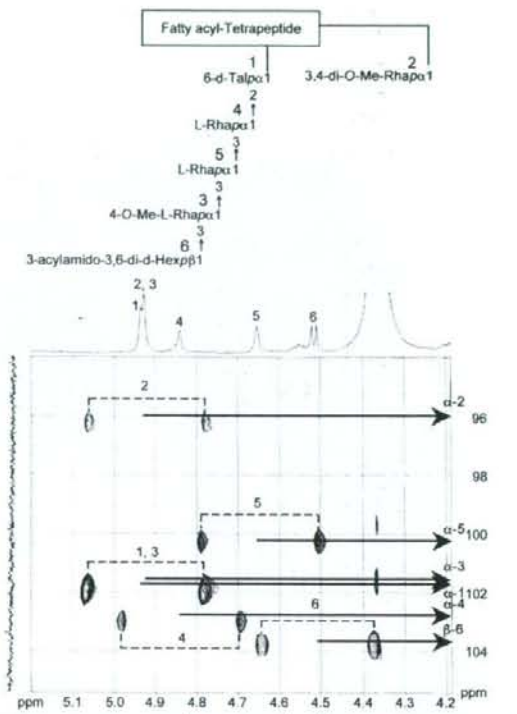

FIG. 6. Nondecoupled ^{1}H-detected [^{1}H, ^{13}C] HMQC spectrum of serotype 16 GPL. Cross-peak labels correspond to those shown on the structure.

serotype 17 GPL was 3-2′-methyl-3′-hydroxy-butanoyl-amido-3,6-dideoxy-β-D-Glc-(1→3)-4-*O*-methyl-α-L-Rha-(1→3)-α-L-Rha-(1→3)-α-L-Rha-(1→2)-6-d-L-Tal (9, 25). Based on the behavior of GPLs in TLC and the GC-MS analysis of alditol acetate derivatives, serotype 16 GPL seems to possess a unique carbohydrate epitope similar to that of serotype 17 GPL. We compared the OSE of serotype 16 GPL to that of serotype 17 GPL. The acylated amido group that was bound to the terminal sugar was different, although the linkage position was identical. Except for the terminal-acylated amido sugar, the other sugar compositions and glycosyl linkage positions were completely identical. An acylated amido group attached to the C-3 position of Hex is very unusual. To our knowledge, 3-amido-Hex is irregular in nature, although 2-amido-Hex is known to be glucosamine or galactosamine, which is frequently isolated as a component of lipopolysaccharides and glycosaminoglycans in prokaryotic and eukaryotic cells (7, 42). Further, existence of short-chain fatty acid 2-methyl-3-hydroxy-4-methoxy-pentanoic acid linked to the amido group of d-Hex is also unique. The characteristic gene cluster is thought to regulate the production of 3-acylated-amido-Hex. It is difficult to determine the species of acylated amido sugars, because no reference standard is available. The terminal sugar of the serotype 17 GPL was reviewed as a gluco-configuration, although firm evidence was not shown (9, 25). The J_{CH} and $J_{1,2}$ values for the anomeric proton in the terminal sugar were 161 and 7.7 Hz,

TABLE 1. Similarity to protein sequences of ORFs in cosmid clone no. 253 derived from *M. intracellulare* serotype 16 strain ATCC 13950^T

ORF	Predicted molecular mass (kDa)	Predicted pI	Exhibits similarity to:	E value	Amino acid identity (no. matched/total no.)	Accession no.
GtfB	45.6	6.35	Glycosyltransferase GtfB	0.0	417/418	BAF45360
Orf 1	45.2	6.10	Putative glycosyltransferase	0.0	416/417	BAF45361
Orf 2	78.9	8.51	Putative acyltransferase	0.0	557/728	BAF45368
Orf 3	31.0	5.88	Putative methyltransferase	2e-89	382/421	NP_218045
Orf 4	15.7	4.94	Conserved hypothetical protein	1e-39	73/129	BAD50406
Orf 5	16.0	4.69	Conserved hypothetical protein	5e-40	75/135	EAX55190
Orf 6	41.1	5.88	Aminotransferase/DegT_DnrJ_EryC1	6e-119	208/357	ABD68440
Orf 7	40.6	9.65	Conserved hypothetical protein	2e-89	178/304	AAS03547
Orf 8	36.7	5.32	Conserved hypothetical protein	2e-52	116/298	CAE06954
Orf 9	22.3	9.79	Putative *N*-acetyltransferase	4e-14	58/166	EAU11841
Orf 10	25.3	7.82	Short-chain dehydrogenase/reductase	7e-47	101/233	EAO61220
Orf 11	23.8	6.05	Putative hydrolase	4e-24	64/196	ABG85599
Orf 12	37.2	6.50	Ketoacyl-acyl carrier protein synthase III	3e-55	126/331	EAX48715
Orf 13	42.5	7.72	Short-chain dehydrogenase/reductase	2e-42	97/248	ZP_01289005
Orf 14	65.8	4.70	Predicted enzyme involved in methoxymalonyl-acyl carrier protein biosynthesis	6e-85	201/575	ABB73590
Orf 15	50.0	6.23	Acyl coenzyme A synthetases	2e-128	233/445	EAT27362
Orf 16	39.1	8.00	Putative glycosyltransferase	2e-106	196/318	NP_855197
Orf 17	37.7	9.46	Putative glycosyltransferase	8e-160	278/323	BAF45369
DrrC	28.6	11.47	Daunorubicin resistance protein C	6e-132	233/261	BAF45370

respectively (Fig. 6; Table S1 in the supplemental material). These results demonstrated unequivocally that the terminal amido-Hex was β configuration and H-2 was in the axial position. The terminal amido-Hex is considered to be derived from glucose or galactose, not Rha.

Next, we explored the genetic mechanism of GPL biosynthesis, because the elongation of carbohydrate chains in serotype-specific GPLs is poorly understood. The *ser2* gene cluster of the *M. avium* serotype 2 strain (31) and a 27.5-kb DNA fragment of the *M. avium* serotype 4 strain (28) were identified to be responsible for the biosynthesis of each OSE in GPLs. Recently, enzymatic characterizations of glycosyltransferase and methyltransferase of nonpolar GPLs have been reported for *Mycobacterium smegmatis* (36, 38). In the serotype-specific polar GPL biosynthesis of MAC, only the *rfA* gene was functionally clarified to encode the transfer of L-Rha to 6-d-Tal, but which gene cluster transfers the sugars next to L-Rha elongated from 6-d-Tal is unclear.

In this study, we cloned the biosynthetic cluster of the serotype 16 GPL and analyzed its sequence. Seventeen ORFs were detected in the serotype 16 strain, and the sequence homology was analyzed. The transformant of the *M. avium* serotype 1

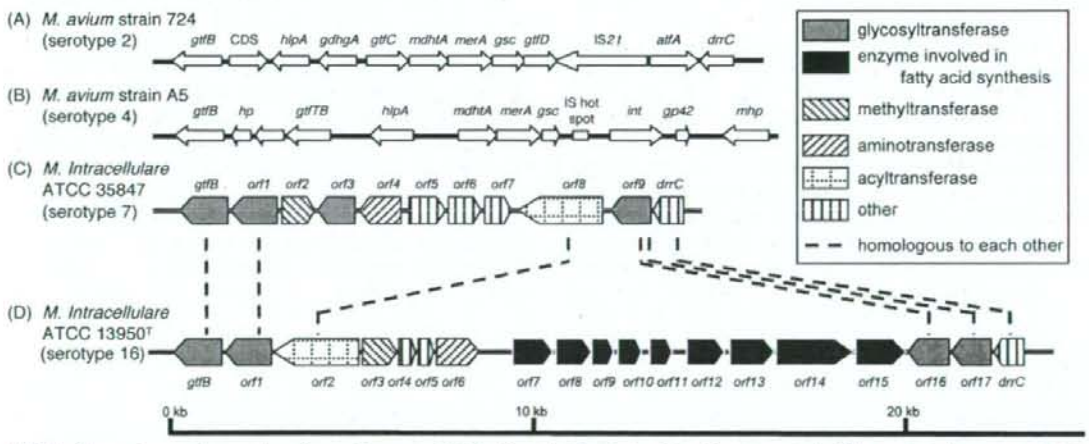

FIG. 7. Comparison and overview of genetic maps of GPL biosynthetic cluster. The *M. avium* strain 724 annotated sequence obtained from GenBank (accession no. AF125999) (A); the *M. avium* strain A5 annotated sequence obtained from GenBank (accession no. AY130970) (B); the *M. intracellulare* ATCC 35847 sequenced in our previous study (GenBank accession no. AB274811) (C); the *M. intracellulare* ATCC 13950^T sequenced in this study (GenBank accession no. AB355138) (D). The orientation of each gene is shown by the direction of the arrow. In panels A and B, putative ORFs not showing homology to known proteins sequences are not depicted. The sequences extending upstream in panels A and B and downstream in panel B are not included in the figure.

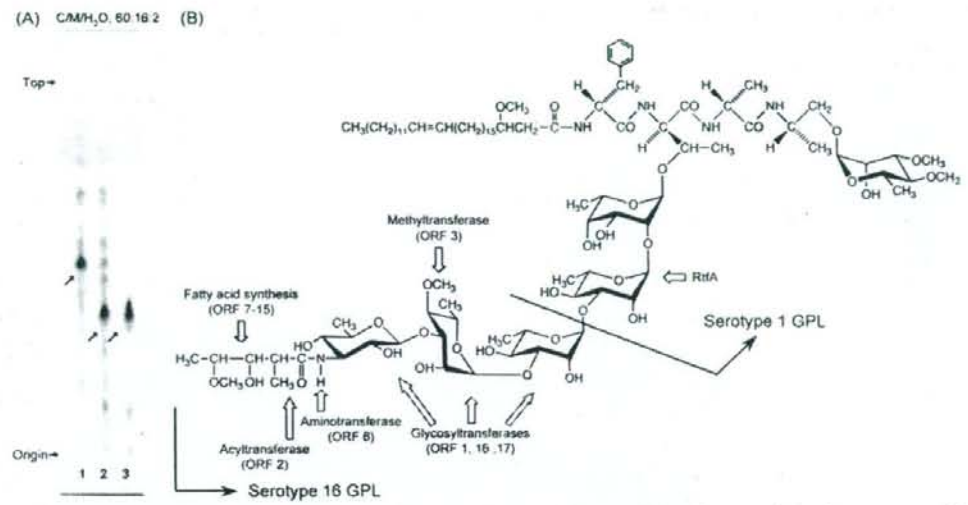

FIG. 8. TLC pattern of *M. avium* serotype 1 and its transformant with cosmid clone no. 253 and proposed complete structure of the serotype 16 GPL. (A) The alkaline-stable lipids derived from *M. avium* serotype 1 (lane 1), its transformant (lane 2), and purified serotype 16 GPL (lane 3) were developed with the solvent system of chloroform-methanol-water (60:16:2, vol/vol/vol). (B) Predicted biosynthesis gene clusters are indicated by arrows.

strain carrying cosmid clone no. 253 produced serotype 16 GPL. These results strongly implied that this *gtfB-drrC* region is responsible for the biosynthesis of the serotype 16-specific GPL. From the structural analysis of the serotype 16 GPL and the sequence of cosmid clone no. 253, it is possible to predict the relationship between the biosynthesis of serotype 16 GPL and the function of each ORF.

The genetic map of the serotype 16 GPL biosynthetic cluster was compared to those of serotype 2 GPL from *M. avium* strain 724, serotype 4 GPL from *M. avium* strain A5, and serotype 7 GPL from *M. intracellulare* strain ATCC 35847^T (12, 18, 28). Significant differences were found in the neighborhood of the conserved region. The genetic organization of the serotype 16 GPL gene cluster was distinct from that of serotype 7, except for some of the ORFs, and the ORFs in this region of serotype 2 and serotype 4 were completely different from ORFs 1 to 17 in serotype 16 (Fig. 7).

In addition to *M. intracellulare* serotype 7 (18) and serotype 16 strains, we have analyzed similar gene clusters of *M. intracellulare* serotype 12 and 17 strains. The sequence homology of the regions of ORF 1 and ORF 17 was highly conserved between only *M. intracellulare* serotype 16 and 17 strains (unpublished data). ORFs 1, 16, and 17 may lead to transfer of the two additional molecules of L-Rha and terminal amido-Hex. ORF 2 was assigned to acyltransferase and may be responsible for biosynthesis of the 3-2′-methyl-3′-hydroxy-4′-methoxy-pentanoyl-amido group in the terminal Hex. ORF 3 is probably responsible for the transfer of the *O*-methyl group at the C-4 position in the third L-Rha from 6-d-Tal. ORF 6 is homologous to aminotransferase and possibly associated with the biosynthesis of an amido group in the terminal Hex. The deduced amino acid sequences of ORF 6 in serotype 16 and ORF 4 in serotype 7 have homologies to DegT_DnrJ_EryC1 aminotransferases. However, these two ORFs are dissimilar to each other. Serotype 16 and 7 GPLs have an amido group at the terminal Hex, although the attachment position is different. The serotype 7 GPL has an amido group at the C-4 position in the terminal Hex, but the serotype 16 GPL has it at the C-3 position. Nine ORFs between ORF 7 and ORF 15 are possibly involved in fatty acid synthesis of the acyl chain moiety linked by an amido bond of the terminal Hex. Taken together, this gene cluster may participate in the biosynthetic pathway of the serotype 16-specific GPL, although further study is needed to clarify the function of each ORF.

Recent studies suggest that GPLs play an important role in the phenotype and pathogenicity of MAC. The colony morphology is considered to be influenced by cell wall GPL. MAC colony phenotypes spontaneously occur from smooth to rough type, and this is due to a mutation lacking GPL (3, 13, 22). The deletion of genomic regions encoding GPL biosynthesis may result in the loss of GPL. Danelishvili et al. demonstrated that the uptake by and growth in macrophages of a MAC mutant with the gene belonging to the GPL synthesis pathway inactivated by transposon insertion were decreased (11). Bhatnagar and Schorey have reported that macrophages infected with MAC release exosomes containing GPLs that result in the transfer of the GPLs to uninfected macrophages and induce a proinflammatory response (4). These findings imply that GPL participates in the pathogenicity of MAC. By contrast, our previous studies have demonstrated that anti-GPL antibodies are detected in the sera of most immunocompetent patients with MAC pulmonary disease and that the detection of anti-GPL antibody is useful for the serodiagnosis of MAC disease (15, 26, 27).

To understand the role of GPLs in MAC and its hosts, it is necessary to define the chemical structure and biosynthesis pathways of GPLs. Elucidation of the structure-function relationship of GPL may open a new avenue for controlling MAC disease.

ACKNOWLEDGMENTS

This work was supported by grants from the Ministry of Education, Culture, Sports, Science, and Technology of Japan, the Japan Health Sciences Foundation, and the Ministry of Health, Labor, and Welfare of Japan (Research on Emerging and Reemerging Infectious Diseases).

We are grateful to Sumihiro Hase (Department of Chemistry, Graduate School of Science, Osaka University, Osaka, Japan) and Hiromi Murakami (Osaka Municipal Technical Research Institute, Osaka, Japan) for helpful discussion.

REFERENCES

1. **Baess, I.** 1983. Deoxyribonucleic acid relationships between different serovars of *Mycobacterium avium*, *Mycobacterium intracellulare* and *Mycobacterium scrofulaceum*. Acta Pathol. Microbiol. Immunol. Scand. **91:**201–203.
2. **Barrow, W. W., T. L. Davis, E. L. Wright, V. Labrousse, M. Bachelet, and N. Rastogi.** 1995. Immunomodulatory spectrum of lipids associated with *Mycobacterium avium* serovar 8. Infect. Immun. **63:**126–133.
3. **Belisle, J. T., K. Klaczkiewicz, P. J. Brennan, W. R. Jacobs, Jr., and J. M. Inamine.** 1993. Rough morphological variants of *Mycobacterium avium*. Characterization of genomic deletions resulting in the loss of glycopeptidolipid expression. J. Biol. Chem. **268:**10517–10523.
4. **Bhatnagar, S., and J. S. Schorey.** 2007. Exosomes released from infected macrophages contain *Mycobacterium avium* glycopeptidolipids and are proinflammatory. J. Biol. Chem. **282:**25779–25789.
5. **Bhatt, A., N. Fujiwara, K. Bhatt, S. S. Gurcha, L. Kremer, B. Chen, J. Chan, S. A. Porcelli, K. Kobayashi, G. S. Besra, and W. R. Jacobs, Jr.** 2007. Deletion of *kasB* in *Mycobacterium tuberculosis* causes loss of acid-fastness and subclinical latent tuberculosis in immunocompetent mice. Proc. Natl. Acad. Sci. USA **104:**5157–5162.
6. **Brennan, P. J., and H. Nikaido.** 1995. The envelope of mycobacteria. Annu. Rev. Biochem. **64:**29–63.
7. **Campo, G. M., S. Campo, A. M. Ferlazzo, R. Vinci, and A. Calatroni.** 2001. Improved high-performance liquid chromatographic method to estimate aminosugars and its application to glycosaminoglycan determination in plasma and serum. J. Chromatogr. B **765:**151–160.
8. **Chatterjee, D., G. O. Aspinall, and P. J. Brennan.** 1987. The presence of novel glucuronic acid-containing, type-specific glycolipid antigens within *Mycobacterium* spp. Revision of earlier structures. J. Biol. Chem. **262:**3528–3533.
9. **Chatterjee, D., and K. H. Khoo.** 2001. The surface glycopeptidolipids of mycobacteria: structures and biological properties. Cell. Mol. Life Sci. **58:** 2018–2042.
10. **Daffe, M., and P. Draper.** 1998. The envelope layers of mycobacteria with reference to their pathogenicity. Adv. Microb. Physiol. **39:**131–203.
11. **Danelishvili, L., M. Wu, B. Stang, M. Harriff, S. Cirillo, J. Cirillo, R. Bildfell, B. Arbogast, and L. E. Bermudez.** 2007. Identification of *Mycobacterium avium* pathogenicity island important for macrophage and amoeba infection. Proc. Natl. Acad. Sci. USA **104:**11038–11043.
12. **Eckstein, T. M., J. T. Belisle, and J. M. Inamine.** 2003. Proposed pathway for the biosynthesis of serovar-specific glycopeptidolipids in *Mycobacterium avium* serovar 2. Microbiology **149:**2797–2807.
13. **Eckstein, T. M., J. M. Inamine, M. L. Lambert, and J. T. Belisle.** 2000. A genetic mechanism for deletion of the *ser2* gene cluster and formation of rough morphological variants of *Mycobacterium avium*. J. Bacteriol. **182:** 6177–6182.
14. **Eckstein, T. M., F. S. Silbaq, D. Chatterjee, N. J. Kelly, P. J. Brennan, and J. T. Belisle.** 1998. Identification and recombinant expression of a *Mycobacterium avium* rhamnosyltransferase gene (*rtfA*) involved in glycopeptidolipid biosynthesis. J. Bacteriol. **180:**5567–5573.
15. **Enomoto, K., S. Oka, N. Fujiwara, T. Okamoto, Y. Okuda, R. Maekura, T. Kuroki, and I. Yano.** 1998. Rapid serodiagnosis of *Mycobacterium avium-intracellulare* complex infection by ELISA with cord factor (trehalose 6, 6′-dimycolate), and serotyping using the glycopeptidolipid antigen. Microbiol. Immunol. **42:**689–696.
16. **Falkinham, J. O., III.** 1996. Epidemiology of infection by nontuberculous mycobacteria. Clin. Microbiol. Rev. **9:**177–215.
17. **Field, S. K., D. Fisher, and R. L. Cowie.** 2004. *Mycobacterium avium* complex pulmonary disease in patients without HIV infection. Chest **126:**566–581.
18. **Fujiwara, N., N. Nakata, S. Maeda, T. Naka, M. Doe, I. Yano, and K. Kobayashi.** 2007. Structural characterization of a specific glycopeptidolipid containing a novel *N*-acyl-deoxy sugar from *Mycobacterium intracellulare* serotype 7 and genetic analysis of its glycosylation pathway. J. Bacteriol. **189:**1099–1108.
19. **Gerwig, G. J., J. P. Kamerling, and J. F. G. Vliegenthart.** 1978. Determination of the D and L configuration of neutral monosaccharides by high-resolution capillary G.L.C. Carbohydr. Res. **62:**349–357.
20. **Hakomori, S.** 1964. A rapid permethylation of glycolipid, and polysaccharide catalyzed by methylsulfinyl carbanion in dimethyl sulfoxide. J. Biochem. (Tokyo) **55:**205–208.
21. **Heidelberg, T., and O. R. Martin.** 2004. Synthesis of the glycopeptidolipid of *Mycobacterium avium* serovar 4: first example of a fully synthetic C-mycoside GPL. J. Org. Chem. **69:**2290–2301.
22. **Howard, S. T., E. Rhoades, J. Recht, X. Pang, A. Alsup, R. Kolter, C. R. Lyons, and T. F. Byrd.** 2006. Spontaneous reversion of *Mycobacterium abscessus* from a smooth to a rough morphotype is associated with reduced expression of glycopeptidolipid and reacquisition of an invasive phenotype. Microbiology **152:**1581–1590.
23. **Kaufmann, S. H.** 2001. How can immunology contribute to the control of tuberculosis? Nat. Rev. Immunol. **1:**20–30.
24. **Khoo, K. H., D. Chatterjee, A. Dell, H. R. Morris, P. J. Brennan, and P. Draper.** 1996. Novel *O*-methylated terminal glucuronic acid characterizes the polar glycopeptidolipids of *Mycobacterium habana* strain TMC 5135. J. Biol. Chem. **271:**12333–12342.
25. **Khoo, K. H., E. Jarboe, A. Barker, J. Torrelles, C. W. Kuo, and D. Chatterjee.** 1999. Altered expression profile of the surface glycopeptidolipids in drug-resistant clinical isolates of *Mycobacterium avium* complex. J. Biol. Chem. **274:**9778–9785.
26. **Kitada, S., R. Maekura, N. Toyoshima, N. Fujiwara, I. Yano, T. Ogura, M. Ito, and K. Kobayashi.** 2002. Serodiagnosis of pulmonary disease due to *Mycobacterium avium* complex with an enzyme immunoassay that uses a mixture of glycopeptidolipid antigens. Clin. Infect. Dis. **35:**1328–1335.
27. **Kitada, S., Y. Nishiuchi, T. Hiraga, N. Naka, H. Hashimoto, K. Yoshimura, K. Miki, M. Miki, M. Motone, T. Fujikawa, K. Kobayashi, I. Yano, and R. Maekura.** 2007. Serological test and chest computed tomography findings in patients with *Mycobacterium avium* complex lung disease. Eur. Respir. J. **29:**1217–1223.
28. **Krzywinska, E., and J. S. Schorey.** 2003. Characterization of genetic differences between *Mycobacterium avium* subsp. avium strains of diverse virulence with a focus on the glycopeptidolipid biosynthesis cluster. Vet. Microbiol. **91:**249–264.
29. **Maekura, R., Y. Okuda, A. Hirotani, S. Kitada, T. Hiraga, K. Yoshimura, I. Yano, K. Kobayashi, and M. Ito.** 2005. Clinical and prognostic importance of serotyping *Mycobacterium avium-Mycobacterium intracellulare* complex isolates in human immunodeficiency virus-negative patients. J. Clin. Microbiol. **43:**3150–3158.
30. **Marras, T. K., and C. L. Daley.** 2002. Epidemiology of human pulmonary infection with nontuberculous mycobacteria. Clin. Chest Med. **23:**553–567.
31. **Maslow, J. N., V. R. Irani, S. H. Lee, T. M. Eckstein, J. M. Inamine, and J. T. Belisle.** 2003. Biosynthetic specificity of the rhamnosyltransferase gene of *Mycobacterium avium* serovar 2 as determined by allelic exchange mutagenesis. Microbiology **149:**3193–3202.
32. **McClatchy, J. K.** 1981. The seroagglutination test in the study of nontuberculous mycobacteria. Rev. Infect. Dis. **3:**867–870.
33. **McCloskey, J. A.** 1969. Mass spectrometry, p. 402. *In* J. M. Lowenstein (ed.), Methods in enzymology: lipid, vol. 14. Academic Press, New York, NY.
34. **McNeil, M., H. Gaylord, and P. J. Brennan.** 1988. *N*-formylkansosaminyl-(1-3)-2-*O*-methyl-D-rhamnopyranose: the type-specific determinant of serovariant 14 of the *Mycobacterium avium* complex. Carbohydr. Res. **177:**185–198.
35. **McNeil, M., A. Y. Tsang, and P. J. Brennan.** 1987. Structure and antigenicity of the specific oligosaccharide hapten from the glycopeptidolipid antigen of *Mycobacterium avium* serotype 4, the dominant *Mycobacterium* isolated from patients with acquired immune deficiency syndrome. J. Biol. Chem. **262:** 2630–2635.
36. **Miyamoto, Y., T. Mukai, N. Nakata, Y. Maeda, M. Kai, T. Naka, I. Yano, and M. Makino.** 2006. Identification and characterization of the genes involved in glycosylation pathways of mycobacterial glycopeptidolipid biosynthesis. J. Bacteriol. **188:**86–95.
37. **Odham, G., and E. Stenhagen.** 1972. Fatty acids, p. 211–228. *In* G. R. Waller (ed.), Biochemical application of mass spectrometry. Wiley-Interscience, New York, NY.
38. **Patterson, J. H., M. J. McConville, R. E. Haites, R. L. Coppel, and H. Billman-Jacobe.** 2000. Identification of a methyltransferase from *Mycobacterium smegmatis* involved in glycopeptidolipid synthesis. J. Biol. Chem. **275:**24900–24906.
39. **Supply, P., E. Mazars, S. Lesjean, V. Vincent, B. Gicquel, and C. Locht.** 2000. Variable human minisatellite-like regions in the *Mycobacterium tuberculosis* genome. Mol. Microbiol. **36:**762–771.
40. **Tsang, A. Y., J. C. Denner, P. J. Brennan, and J. K. McClatchy.** 1992. Clinical and epidemiological importance of typing of *Mycobacterium avium* complex isolates. J. Clin. Microbiol. **30:**479–484.
41. **Wayne, L. G., and H. A. Sramek.** 1992. Agents of newly recognized or infrequently encountered mycobacterial diseases. Clin. Microbiol. Rev. **5:**1–25.
42. **Woods, A., and J. R. Couchman.** 2001. Proteoglycan isolation and analysis, p. 10.7.1–10.7.19. *In* J. S. Bonifacino, M. Dasso, J. B. Harford, J. Lippincott-Schwartz, and K. M. Yamada (ed.), Current protocols in cell biology. Wiley Interscience, Hoboken, NJ.

CLINICAL AND VACCINE IMMUNOLOGY, Dec. 2008, p. 1755–1759 Vol. 15, No. 12
1556-6811/08/$08.00+0 doi:10.1128/CVI.00148-08

Serological Diagnosis of Leprosy in Patients in Vietnam by Enzyme-Linked Immunosorbent Assay with *Mycobacterium leprae*-Derived Major Membrane Protein II[▽]

Masanori Kai,[1]* Nhu Ha Nguyen Phuc,[2] Thuy Huong Hoang Thi,[2] An Hoang Nguyen,[2] Yasuo Fukutomi,[1] Yumi Maeda,[1] Yuji Miyamoto,[1] Tetsu Mukai,[1] Tsuyoshi Fujiwara,[3] Tan Thanh Nguyen,[2] and Masahiko Makino[1]

Department of Microbiology, Leprosy Research Center, National Institute of Infectious Diseases, 4-2-1 Aoba-cho, Higashimurayama, Tokyo 189-0002, Japan[1]; Quyhoa National Leprosy & Dermato-Venereology Hospital, Ghenhrang District, Quynhon City, Binhdinh, Vietnam[2]; and Institute for Natural Science, Nara University, Nara 631-8502, Japan[3]

Received 21 April 2008/Returned for modification 13 June 2008/Accepted 12 October 2008

A serological diagnostic test using phenolic glycolipid-I (PGL-I) developed in the 1980s is commercially available, but the method is still inefficient in detecting all forms of leprosy. Therefore, more-specific and -reliable serological methods have been sought. We have characterized major membrane protein II (MMP-II) as a candidate protein for a new serological antigen. In this study, we evaluated the effectiveness of the enzyme-linked immunosorbent assay (ELISA) using the MMP-II antigen (MMP-II ELISA) for detecting antibodies in leprosy patients and patients' contacts in the mid-region of Vietnam and compared to the results to those for the PGL-I method (PGL-I ELISA). The results showed that 85% of multibacillary patients and 48% of paucibacillary patients were positive by MMP-II ELISA. Comparison between the serological tests showed that positivity rates for leprosy patients were higher with MMP-II ELISA than with PGL-I ELISA. Household contacts (HHCs) showed low positivity rates, but medical staff members showed comparatively high positivity rates, with MMP-II ELISA. Furthermore, monitoring of results for leprosy patients and HHCs showed that MMP-II is a better index marker than PGL-I. Overall, the epidemiological study conducted in Vietnam suggests that serological testing with MMP-II would be beneficial in detecting leprosy.

Leprosy is a chronic infectious disease caused by *Mycobacterium leprae* infection, which sometimes leads to progressive peripheral nerve injury and systematic deformity (16, 30). Early detection of *M. leprae* infection and early start of treatment are key in avoiding deformities. Also, in order to decrease the incidence of new cases, it is important to find and treat the sources of the infection as soon as possible. Thus, early detection of these infected individuals who cannot be clinically diagnosed is critical (34). The diagnosis of leprosy is based on microscopic detection of acid-fast bacilli in skin smears or biopsies, along with clinical and histopathological evaluation of suspected patients. Recently, diagnostic methods for leprosy based on *M. leprae* DNA sequences have been developed (10, 20, 25). However, it is difficult to use these methods in developing countries which still have leprosy hot spot areas, because such methods require expensive machines and materials as well as skilled technicians. Although many developing countries have recently established laboratories for DNA-based diagnosis, it is harder to perform DNA tests than serodiagnostic tests. Thus, in countries where leprosy is endemic, diagnosis still relies on clinical observations and easy, inexpensive tests.

Serodiagnosis is generally accepted as the easiest way of diagnosing a disease. For leprosy serodiagnosis, the only antigen currently used is phenolic glycolipid I (PGL-I), which is supposedly specific to *M. leprae* (21, 26, 27). Since the identification of PGL-I in 1981 by Hunter and Brennan (14), a number of serological tools have been developed. Simple assays, such as the Serodia-Leprae method, a dipstick assay, and lateral flow tests based on the PGL-I antigen, have been used to detect leprosy patients in areas where leprosy is endemic (3, 15, 17, 32). However, these tests seem to be insufficient for detection of both multibacillary (MB) and paucibacillary (PB) patients, as well as for early diagnosis, and have not been used as widely as would be expected in field situations (6, 29). Therefore, we have begun the search for a more sensitive antigen. Major membrane protein II (MMP-II; encoded by the ML2038c gene, named *bfrA*, also known as bacterioferritin) was previously identified from the cell membrane fraction of *M. leprae* as an antigenic molecule capable of activating both antigen-presenting cells and T cells (19, 24). A homology search of the mycobacteria nucleotide database revealed that MMP-II is conserved between *M. leprae*, *M. tuberculosis*, and *M. avium*. The amino acid identity is about 86% among the three species. However, we have previously examined the role of MMP-II in the humoral responses of Japanese patients and showed that MMP-II could contribute to the specific serodetection of leprosy patients (18).

In the present study, we performed a serological test using serum samples collected in regions of leprosy endemicity in Vietnam and evaluated the use of MMP-II as an antigen for serodiagnosis of leprosy. We believe that identifying the appropriate antigens for serodiagnosis could facilitate the devel-

* Corresponding author. Mailing address: Department of Microbiology, Leprosy Research Center, National Institute of Infectious Diseases, 4-2-1 Aoba-cho, Higashimurayama, Tokyo 189-0002, Japan. Phone: 81-42-391-8211. Fax: 81-42-391-8807. E-mail: mkai@nih.go.jp.

▽ Published ahead of print on 22 October 2008.

opment of simple diagnostic tests, like dip-stick assays, for use in developing countries.

MATERIALS AND METHODS

Serum samples. A total of 974 serum samples from various individuals, including in- and out-patients of Quyhoa National Leprosy & Dermato-Venereology Hospital (NDH), were obtained under informed consent. The sera were donated by 205 leprosy patients (163 patients undergoing treatment and 42 new patients), 428 household contacts (HHCs), 130 medical staff members, and 211 noncontact healthy individuals. Sera of leprosy patients and their contacts were taken at regional medical centers in the midregion of Vietnam, including those in the Danang, Quangnam, Quangngai, Binhdinh, Phuyen, Khanhhoa, Ninhthuan, Gialai, Kontum, Daklak, and Daknong provinces, where the average prevalence rate is 0.17 (number of cases/10,000 persons) and the average detection rate is 2.13 (number of cases/10,000 persons). Among these provinces, Binhdinh, Ninhthuan, Gialai, and Kontum had hot spot areas. The medical staff members consisted of workers in Quyhoa NDH, including medical doctors, nurses, pharmacists, technicians, and helpers. Only the sera from medical staff members who were not HHCs of leprosy patients were used in this study. Sera were also obtained from healthy persons living in the Binhdinh province (n = 126) and the Longan province (n = 85), which are distantly located from each other. Out of 205 leprosy patients, 121 had MB leprosy and 84 had PB leprosy. We made the initial diagnosis according to the Ridley-Jopling classification system and classified patients as MB and PB types based on the WHO recommendation. In Vietnam, the *M. bovis* bacille Calmette-Guérin (BCG) vaccination against tuberculosis has been undertaken in earnest since 1976. Almost all medical staff personnel who donated their blood for this study were vaccinated with BCG.

MMP-II and PGL-I antigens. The MMP-II gene (ML2038c, or *bfrA*) was expressed in *Escherichia coli* as a fusion construct by using a pMAL-c2X expression vector (New England BioLabs) (18). Synthetic bovine serum albumin-conjugated trisaccharide-phenyl propionate for the detection of PGL-I antibodies was produced by our laboratory. The procedure for synthesis of the antigen is described elsewhere (12).

ELISAs for detection of antibodies. MaxiSorp (Nalge Nunc) microtiter plates were coated with 50 μl antigen solution (MMP-II [0.4 μg/ml] and PGL-I [0.2 μg/ml]) in carbonate-bicarbonate buffer (pH 9.4) and kept at 4°C overnight. The optimal concentrations of these antigens were determined in advance. The enzyme-linked immunosorbent assay (ELISA) protocol was performed as described previously (18). We measured anti-MMP-II immunoglobulin G (IgG) antibodies and anti-PGL-I IgM antibodies. Plate-to-plate variations in optical density (OD) readings were controlled for by using a common standard serum.

Monitoring. One hundred forty-eight leprosy patients have been monitored using MMP-II ELISA and PGL-I ELISA during their multidrug therapy (MDT) treatment since 2001. Twelve-month MDT for MB was carried out, and sampling was performed three to five times. Also, HHCs were monitored once every 3 or 6 months by both the MMP-II and the PGL-I ELISA methods from 2001 to 2004.

Statistics. The data were analyzed using a statistical software package (version 9.3.2.0; MedCalc software). A receiver operator characteristic (ROC) curve was drawn to calculate the cutoff levels (2). Additionally, the statistically significant differences between assays were confirmed by the chi-square test (28).

RESULTS

Comparison of the distribution of ELISA values between MMP-II and PGL-I. We focused on the distribution of ELISA values derived from MB leprosy patients and compared them to those from healthy individuals (Fig. 1). The cutoff OD_{405} value for anti-MMP-II antibody was defined as 0.103 (95% confidence interval, 85.2 to 93.7), and that for anti-PGL-I antibody was defined as 0.452 (95% CI, 85.2 to 93.7), by ROC curve analysis (MedCalc software) using OD titers from 211 healthy individuals and 205 leprosy patients. The distribution pattern of MMP-II ELISA values was quite different from that of PGL-I ELISA for healthy individuals. While the OD values of most healthy individuals were in the low range for MMP-II ELISA (Fig. 1A), the titers obtained by PGL-I ELISA showed a bell-shaped curve which was similar to that of MB leprosy patients (Fig. 1B). The PGL-I ELISA values for PB leprosy patients also showed a similar bell-shaped curve (data not shown).

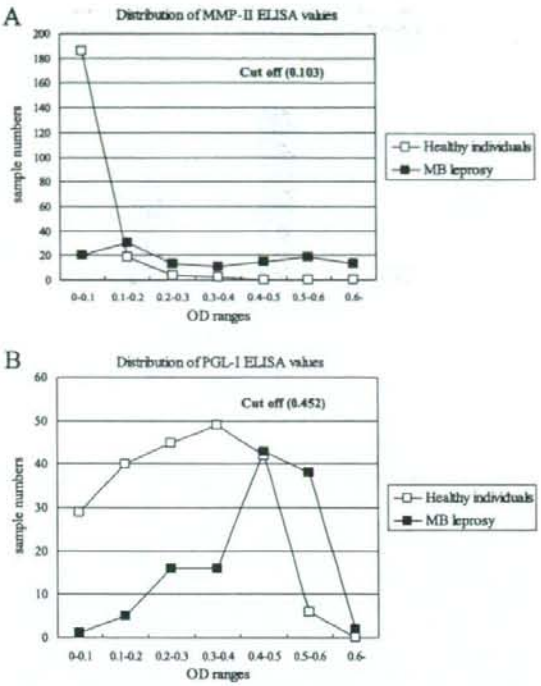

FIG. 1. Comparison of distributions of OD values in MB leprosy patients and normal individuals. (A) Distribution pattern of MMP-II ELISA values in patients and healthy individuals. (B) Distribution pattern of PGL-I ELISA values in patients and healthy individuals. The solid squares show the number of MB leprosy patients in each OD value range, and the open squares show the number of healthy individuals.

Detection rate of antibodies in sera of leprosy patients. Among the MB patients, 85.1% were positive by MMP-II ELISA and 57.0% were positive by PGL-I ELISA; 47.6% of PB patients were positive by MMP-II ELISA, and 20.2% were positive by PGL-I ELISA (Fig. 2). The MMP-II ELISA values for both MB and PB patients were significantly higher than the PGL-I ELISA values ($P < 0.001$) (Fig. 2). Patients undergoing treatment and new cases showed a similar difference (data not shown).

Seropositivity rates of contacts, medical staff members, and healthy volunteers. There was no significant difference in positivity rate between MMP-II ELISA and PGL-I ELISA for healthy individuals and HHCs (Fig. 3). Also, there was no significant difference in positivity rate between MMP-II ELISA and PGL-I ELISA for healthy individuals from different provinces, namely, Binhdinh and Longan (data not shown). In contrast, the medical staff showed a significantly higher rate of positivity by MMP-II ELISA (26.2%) than by PGL-I ELISA. The anti-MMP-II antibody positivity rate for the medical staff

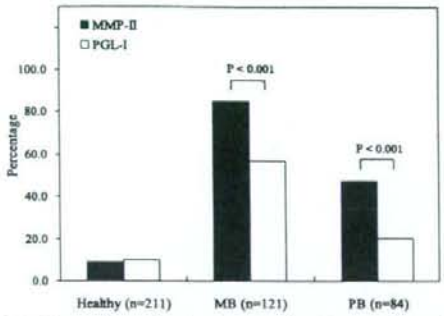

FIG. 2. Comparison of positivity rates of patients as determined by MMP-II and PGL-I ELISA. Black bars show percentages of healthy individuals and patients positive by MMP-II ELISA, and white bars show those for PGL-I ELISA. Statistically significant differences were confirmed by the chi-square test and are indicated as *P* values.

was significantly higher than those for healthy individuals and HHCs.

Monitoring of HHCs. Previous studies suggested the usefulness of PGL-I ELISA in monitoring the effects of leprosy treatment (5, 8, 9, 22). Therefore, we monitored anti-MMP-II antibody titers in patients after treatment and compared them to anti-PGL-I antibody titers. Ninety-two MB and 56 PB patients were monitored. The anti-MMP-II antibody value of approximately 30% of monitored MB patients declined within 1 to 2 years after the start of treatment, in accordance with changes in bacterial index values (data not shown), although approximately 50% of MB patients showed no reduction in ELISA values and 20% of patients showed mild increases in value. Three representative samples of MB patients are shown in Fig. 4. Among PB patients, 18% of the monitored patients had reduced anti-MMP-II antibody titers. On the other hand, anti-PGL-I antibody titers were reduced approximately only 20% in both MB and PB patients during the monitoring period. Therefore, anti-MMP II antibody may reflect the efficacy of treatment similarly to or slightly better than anti-PGL-I antibody in some cases. Furthermore, 9 individuals out of 428

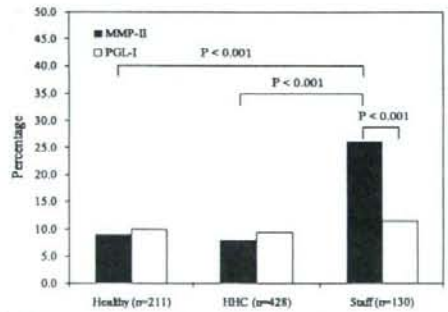

FIG. 3. Positivity rates of HHCs and medical staff members as determined by MMP-II and PGL-I ELISA. Black bars show percentages of HHCs and medical staff members positive by MMP-II ELISA, and white bars show those by PGL-I ELISA. Statistically significant differences were confirmed by the chi-square test and are indicated as *P* values.

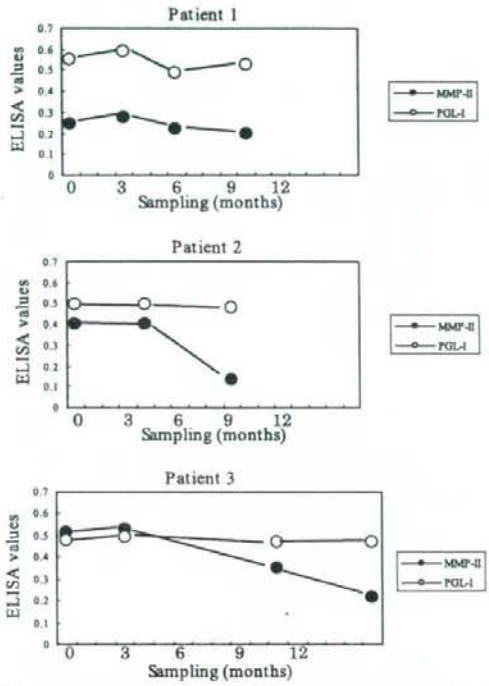

FIG. 4. Monitoring of three MB leprosy patients by MMP-II and PGL-I ELISAs. Three cases of monitored leprosy patients are shown. The closed circles show MMP-II ELISA values, and the open circles show PGL-I ELISA values. Note that the cutoff value for MMP-II is 0.103 and that of PGL-I is 0.452.

HHCs developed leprosy after several years of monitoring. Among the nine cases, two individuals had increasing antibody titers by MMP-II and/or PGL-I ELISA 1 year before manifesting clinical symptoms (data not shown). Patient HHC192 showed a prominent rise in anti-MMP-II antibody values during the asymptomatic period. Both patients developed MB leprosy. The other seven, whose antibody levels did not show an apparent increase during the observation period, developed PB leprosy.

DISCUSSION

Serodiagnosis is the easiest, cheapest, and least invasive diagnostic tool for infectious diseases. Currently, PGL-I is used as a specific antigen for *M. leprae*, but in practice, its sensitivity and specificity are not as high as expected, even though previous studies using stock sera reported that the detection rate for MB patients was more than 80% (1, 3, 4, 7). The present study involving Vietnamese leprosy patients indicated that there is a significant difference between MMP-II ELISA and PGL-I ELISA in detecting both MB and PB leprosy. The positivity rate of anti-MMP-II antibody for MB leprosy was approximately 85%, and that for PB leprosy was 48%; these titers were significantly higher than the titers obtained by PGL-I ELISA (57% and 20%, respectively). The detection rates obtained by

MMP-II ELISA were similar to those for a previous study using stock sera from Japanese leprosy patients (18). However, the positivity rates of anti-PGL-I antibody in the present study were significantly lower than those for the Japanese patients, although the same antigens for both MMP-II and PGL-I were used in the two studies.

There are several possible reasons why the sensitivity of PGL-I ELISA was low in the present study. One reason may be that some healthy Vietnamese individuals have high anti-PGL-I antibody titers. Although we could not conduct further detailed analysis on the subjects, these individuals might be highly exposed to *M. leprae*, and so their B lymphocytes might be repeatedly stimulated with *M. leprae*-derived antigens, including PGL-I. It seems quite difficult to discriminate the healthy individuals from MB or PB leprosy patients by PGL-I ELISA, as shown in Fig. 1. Furthermore, we concluded that a reasonable cutoff point for PGL-I ELISA was an OD_{405} of 0.452, as deduced from Fig. 1 and the ROC values, but this resulted in lower sensitivity. The difference in sensitivity between PGL-I ELISA and MMP-II ELISA may also be due to differences in the biochemical features of the antigens. PGL-I is a glycolipid component, and as such, it might be retained in some infected cells for a long time after the initial exposure (13, 33). This speculation is supported by previous reports showing that healthy individuals residing in areas where leprosy is endemic had high anti-PGL-I antibody titers, and *M. leprae* DNA was recovered by PCR from the nasal swabs of these individuals (31, 32). Also, it has been reported that the usefulness of PGL-I-based tests for early diagnosis is limited, since 7 to 10% of individuals testing positive do not develop the disease (14).

In contrast, MMP-II is a protein antigen and is considered to be one of the immunodominant antigens of *M. leprae* (19). Therefore, in individuals who have been exposed to *M. leprae* but have not developed leprosy, antigen-presenting cells expressing MMP-II might feasibly be eliminated from the body by immune cells such as cytotoxic T lymphocytes and thus lack the ability to produce anti-MMP-II antibodies through antigen-presenting-cell-dependent mechanisms. These speculations seem to be supported by our present observations with sera from patients monitored over time. Anti-MMP-II antibody titers of MB patients declined earlier than PGL-I titers with MDT treatment, indicating the disappearance of MMP-II antigens, while no apparent reduction in PGL-I antigens was observed during the 12 months of observation (Fig. 4). Furthermore, in one case the anti-MMP-II antibody titer increased drastically before manifestation of clinically apparent leprosy (data not shown).

Medical staff members (n = 130) showed a high positivity rate by MMP-II ELISA, compared with healthy individuals or HHCs. These medical staff members were mostly BCG vaccinated, as were the HHCs. Therefore, it seems that BCG vaccination has no effect on anti-MMP-II antibody titers. Although we could not determine a conclusive reason for the high positivity rate, these medical personnel may be repeatedly exposed to *M. leprae* in hospitals. However, we cannot eliminate the possibility that they have produced the antibody in response to exposure to other mycobacteria, since the MMP-II protein is conserved in other pathogenic mycobacterial species, such as *M. tuberculosis* and *M. avium*, though the staff members with high anti-MMP-II antibody titers did not manifest any clinical signs or features indicating infection with other mycobacteria. We tried to perform nested PCR using the *M. leprae*-specific repetitive element for DNA extracted from nasal swabs of some hospital staff members (n = 25). However, because the sampling dates for the serological test and the PCR test were not coordinated, we could not come to a definite conclusion. Nevertheless, we were surprised to find that ≅40% (n = 25) of the nasal swab samples were positive (data not shown). As for tuberculosis, it is said that one-third of the world population is infected with *M. tuberculosis*. The same may be the case with leprosy, although further studies are needed with larger populations, including medical staff members as well as contacts and noncontacts of leprosy.

Taken together, our data indicate that MMP-II ELISA could be useful as a supporting serodiagnostic tool in combination with other clinical diagnostic methods and may also be useful in monitoring disease activity. Furthermore, in this study the correlation between MMP-II and PGL-I was low, with a correlation coefficient among the 205 leprosy patients of only 0.63. If both PGL-I and MMP-II antibodies could be measured simultaneously, the sensitivity of the assay system could be increased. Considering that PGL-I is a sugar antigen (eliciting IgM antibodies) and MMP-II is a protein antigen (eliciting IgG antibodies), assaying for a combination of these antibodies could lead to more-accurate detection of leprosy in the field.

ACKNOWLEDGMENTS

This research was supported in part by Health Sciences research grants for research on emerging and reemerging infectious diseases; by an international cooperation research grant (topic code 18C4) from the Ministry of Health, Labor and Welfare of Japan; and by Quyhoa NDH.

REFERENCES

1. **Agis, F., P. Schlich, J. L. Cartel, C. Guidi, and M. A. Bach.** 1988. Use of anti-*M. leprae* phenolic glycolipid-I antibody detection for early diagnosis and prognosis of leprosy. Int. J. Lepr. Other Mycobact. Dis. **56**:527–535.
2. **Beck, J. R., and E. K. Schultz.** 1986. The use of relative operating characteristic (ROC) curves in test performance evaluation. Arch. Pathol. Lab. Med. **110**:13–20.
3. **Bührer-Sékula, S., H. L. Smits, G. C. Gussenhoven, J. van Leeuwen, S. Amador, T. Fujiwara, P. R. Klatser, and L. Oskam.** 2003. Simple and fast lateral flow test for classification of leprosy patients and identification of contacts with high risk of developing leprosy. J. Clin. Microbiol. **41**:1991–1995.
4. **Cartel, J. L., S. Chanteau, J. P. Boutin, R. Plichart, P. Richez, J. F. Roux, and J. H. Grosset.** 1990. Assessment of anti-phenolic glycolipid-I IgM levels using an ELISA for detection of *M. leprae* infection in populations of the South Pacific Islands. Int. J. Lepr. Other Mycobact. Dis. **58**:512–517.
5. **Chanteau, S., J. L. Cartel, P. Celerier, R. Plichart, S. Desforges, and J. Roux.** 1989. PGL-I antigen and antibody detection in leprosy patients: evolution under chemotherapy. Int. J. Lepr. Other Mycobact. Dis. **57**:735–743.
6. **Chanteau, S., P. Glaziou, C. Plichart, P. Luquiaud, R. Plichart, J. F. Faucher, and J. L. Cartel.** 1993. Low predictive value of PGL-I serology for the early diagnosis of leprosy in family contacts: results of a 10-year prospective field study in French Polynesia. Int. J. Lepr. Other Mycobact. Dis. **61**:533–541.
7. **Chaturvedi, V., S. Sinha, B. K. Girdhar, and U. Sengupta.** 1991. On the value of sequential serology with a *Mycobacterium leprae*-specific antibody competition ELISA in monitoring leprosy chemotherapy. Int. J. Lepr. Other Mycobact. Dis. **59**:32–40.
8. **Cho, S. N., R. V. Cellona, T. T. Fajardo, Jr., R. M. Abalos, E. C. dela Cruz, G. P. Walsh, J. D. Kim, and P. J. Brennan.** 1991. Detection of phenolic glycolipid-I antigen and antibody in sera from new and relapsed lepromatous patients treated with various drug regimens. Int. J. Lepr. Other Mycobact. Dis. **59**:25–31.
9. **Cho, S. N., R. V. Cellona, L. G. Villahermosa, T. T. Fajardo, Jr., M. V. Balagon, R. M. Abalos, E. V. Tan, G. P. Walsh, J. D. Kim, and P. J. Brennan.** 2001. Detection of phenolic glycolipid I of *Mycobacterium leprae* in sera from